Summer 8-16-2021

The Effect of a Ferrite-Core Relay Vs. an Air-Core Relay on the Output Power Characteristics of a Three-Coil Wireless Power Transfer System

Jakob L. White
Portland State University

The Effect of a Ferrite-Core Relay Vs. an Air-Core Relay on the Output Power Characteristics of a Three-Coil Wireless Power Transfer System

An undergraduate honors thesis submitted in partial fulfillment of the requirements for the degree of
Bachelor of Science
in
University Honors
and
Electrical Engineering

Author:
Jakob White

Thesis Advisor:
David Burnett

Date:
August 17, 2021

Maseeh College of Engineering and Computer Science
PORTLAND STATE UNIVERSITY

Abstract

The purpose of this thesis is to determine the effect of using a ferrite-core relay on the output power characteristics of a three-coil, parallel-tuned, domino-resonator wireless power transfer (WPT) system in comparison to the effect of using an air-core relay in such a system. First, a general mathematical model is presented to describe both the ferrite-core-relay system and the air-core-relay system and to calculate their output power characteristics for seven different resistive loads at each of five different distance configurations between the coils. Next, experimental results are analyzed and compared to the mathematical results to confirm model accuracy. Finally, the output power characteristics of the two systems are compared and contrasted. The results of this thesis show that the model is most accurate when working with loads around 1kΩ, exhibiting an error of about 25%. More importantly, maximum power output is achieved when working with loads around 1kΩ, at which the average improvement to output power when using a ferrite core instead of an air core is about 87%. Therefore, it can be concluded that, with coil geometries and operating frequencies being held constant, the inclusion of a ferrite core in relay coils can noticeably improve output power characteristics at a given distance between coils. The reason for this improvement is most probably the result of magnetic flux concentration by the ferrite core, which in turn increases induced current and therefore output power.

Index Terms

Wireless Power Transfer, WPT, Three-Coil, Ferrite-Core, Long-Distance, Parallel-Tuned.

Contents

List of Figures

List of Tables

I Introduction

IN recent years, Wireless Power Transfer (WPT) has become increasingly important for the remote powering of many wireless devices such as wearable electronics, chemical sensors, and communication devices [1]. Generally, the overall objective of any WPT system is to deliver just enough power as efficiently as possible with the greatest degree of freedom of position and orientation between the transmitter and receiver. Still, WPT systems can be classified according to power delivery and transmission distance. A WPT system is either High Power (15W to 100W), Medium Power (5W to 15W), or Wearable (up to 5W) [2], and either Long Range (coil-radius-to-distance ratio is much greater than 3), Medium Range (coil-radius-to-distance ratio is greater than 3), or Short Range (coil-radius-to-distance is ratio less than 3) [3]. In some wearable long-range applications, such as the wireless nodes being developed by Dr. Burnett [4], efficiency isn't nearly as important as maximum power delivery and compactness of the receiver. Several papers have been produced discussing the various options to increase the power delivery in long-range WPT systems, from metamaterials to relays. In regard to the latter, researchers have primarily experimented with series-tuned WPT systems using air-core coils and have not experimented with parallel-tuned WPT systems [5]. Furthermore, while other researchers have shown the promising results of using ferrite cores to increase WPT transmission distance and efficiency, they do not discuss using ferrite cores with the relay coil [6]. Therefore, the objective of this thesis is to determine the effect of using a ferrite-core relay on the output power characteristics of a three-coil, parallel-tuned, domino-resonator wireless power transfer (WPT) system in comparison to the effect of using an air-core relay in such a system.

In order to accomplish this objective, this thesis is divided into three parts. In the first part, a general mathematical model is derived to represent the interactions between the transmitter, relay, and receiver in a three-coil WPT system. This model is then used to derive the theoretical behavior of a Taidacent High Power Long-Distance Wireless Power Supply Module [7] using both an air-core relay and a hollow-cylinder ferrite-core relay. The usage of a hollow-cylinder ferrite core instead of a standard ferrite rod is justified as a compromise between increased power transmission and weight [8]. The output power to each of seven loads between 1Ω and 1MegaΩ at each of five distance configurations between the coils is measured for both the air-core-relay and ferrite-core-relay systems. For each of the distance configurations, the transmitter and receiver coils are placed at a certain distance apart, and the relay is placed at a point where the output voltage is maximum. In the second part, experiments are conducted with a real Taidacent High Power Long-Distance Wireless Power Supply Module to reflect and confirm the calculations of the mathematical model. Finally, in the third part, the mathematical model and experimental results are analyzed and compared to determine model accuracy for both the air-core-relay and ferrite-core-relay systems. These two systems are also compared to each other to determine the effect that a ferrite core has on the output power characteristics relative to a traditional air core. The implication of this research is that a new way of using ferrite cores in WPT systems will be revealed, possibly enabling more-efficient and longer-range WPT for low-power wireless devices.

II System Modeling and Mathematical Analysis

II-A General Model and Math

The general WPT system structure used in this thesis is shown in Fig. 1. The coils are all planar and concentric, and the receiver is simply a parallel-tuned RLC circuit. The only difference between the air-core-relay system and the ferrite-core-relay system is that, to compensate for the change in inductance resulting from the introduction of a ferrite core, the compensation capacitor of the relay is changed in proportion to maintain the same resonant frequency. Coil geometry remains constant. See Tables I and II for parameter definitions.

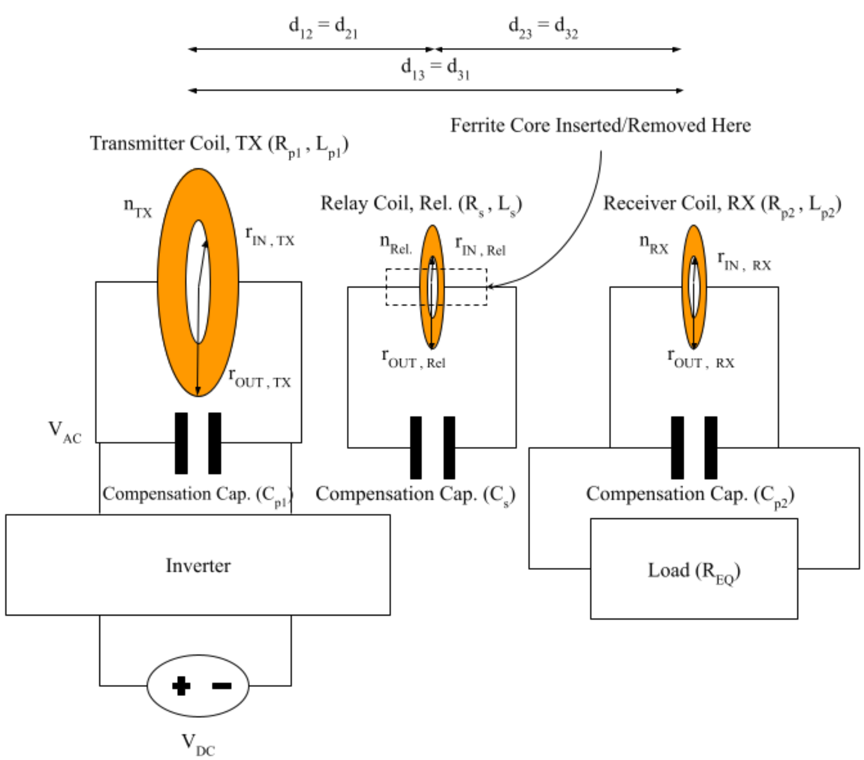

Fig. 1: The General Structure of the WPT System in Question. The ”Inverter” serves to turn the DC power supply voltage into a higher AC voltage at the resonant frequency of the transmitter’s LC circuit.

Geometric Parameters		
Parameter	**Definition**	**Value**
d_{12}, d_{21}	Distance between TX and Rel. Coils	$d_{13} - d_{23}$
d_{13}, d_{31}	Distance between TX and RX Coil	[0.2, 0.4, 0.6, 0.8, 1.0] m
d_{23}, d_{32}	Distance between Rel. and RX Coils	∼15mm to ∼50mm
$r_{out_{TX}}$	Outer Radius of TX Coil	100mm
$r_{out_{Rel.}}$	Outer Radius of Rel. Coil	25mm
$r_{out_{RX}}$	Outer Radius of RX Coil	25mm
$r_{in_{TX}}$	Inner Radius of TX Coil	95mm
$r_{in_{Rel.}}$	Inner Radius of Rel. Coil	15mm
$r_{in_{RX}}$	Inner Radius of RX Coil	15mm
w_{TX}	Width of TX Coil Wire	1.19mm
$w_{Rel.}$	Width of Rel. Coil Wire	0.445mm
w_{RX}	Width of RX Coil Wire	0.445mm
s_{TX}	TX Coil Pitch	0mm
$s_{Rel.}$	Rel. Coil Pitch	0mm
s_{RX}	RX Coil Pitch	0mm
n_{TX}	Number of Turns in TX Coil	5
$n_{Rel.}$	Number of Turns in Rel. Coil	15
n_{RX}	Number of Turns in RX Coil	15
$r_{Out_{Core}}$	Outer Radius of Ferrite Core	15.1mm
$r_{In_{Core}}$	Inner Radius of Ferrite Core	8.95mm
l_{Core}	Length of Ferrite Core	15.4mm
r_s	Average Radius of Relay Coil	20mm
r_f	Radius of Equivalent Ferrite Rod	12.2mm

TABLE I: Geometric Parameters, Their Definitions, and Their Datasheet Values in the Taidacent WPT System

Circuit Parameters		
Parameter	**Definition**	**Value**
V_{DC}	Input DC Power Supply Voltage	24V
V_{AC}	Voltage Across TX LC Circuit	∼100V
R_{p1}	Series Resistance of TX Coil	∼0.02 Ω
L_{p1}	Self Inductance of TX Coil	14 μH
C_{p1}	Compensation Capacitance for TX Coil	39 nF
R_s	Series Resistance of Rel. Coil	∼0.02 Ω
L_s	Self Inductance of Rel. Coil	∼20 μH
C_s	Compensation Capacitance for Rel. Coil	27 nH
R_{p2}	Series Resistance of RX. Coil	∼0.02 Ω
L_{p2}	Self Inductance of RX. Coil	∼20 μH
C_{p2}	Compensation Capacitance for RX. Coil	27 nH
R_{EQ}	Resistive Load	[1 100 100 1000 10000 100000 1000000] Ω
I_1	Current in Lp1	Use Eq. 1
I_2	Current in Lp2	Use Eq. 1
I_3	Current in Lp3	Use Eq. 1
ω	Resonant/Operation Frequency	1.35×10^6 Rad/sec (= 215kHz)
M_{12}	Mut. Ind. between TX and Rel.	Use Eq.'s 2 and 9
M_{21}	Mut. Ind. between Rel. and TX	Use Eq.'s 2 and 9
M_{13}	Mut. Ind. between TX and RX	Use Eq.'s 2 and 9
M_{31}	Mut. Ind. between RX and TX	Use Eq.'s 2 and 9
M_{23}	Mut. Ind. between Rel. and RX	Use Eq.'s 2 and 9
M_{32}	Mut. Ind. between RX and Rel.	Use Eq.'s 2 and 9
$\mu_{core_{avg}}$	Average Permeability of Hollow Cylinder Ferrite Core	1.38

TABLE II: Circuit Parameters, Their Definitions, and Their Datasheet Values in the Taidacent WPT System

The WPT system circuit model used in this thesis is shown in Fig. 2. Using Kirchhoff's Voltage Law, a matrix can be formed and used to solve for the currents in the inductors of the system. See Table I for parameter definitions.

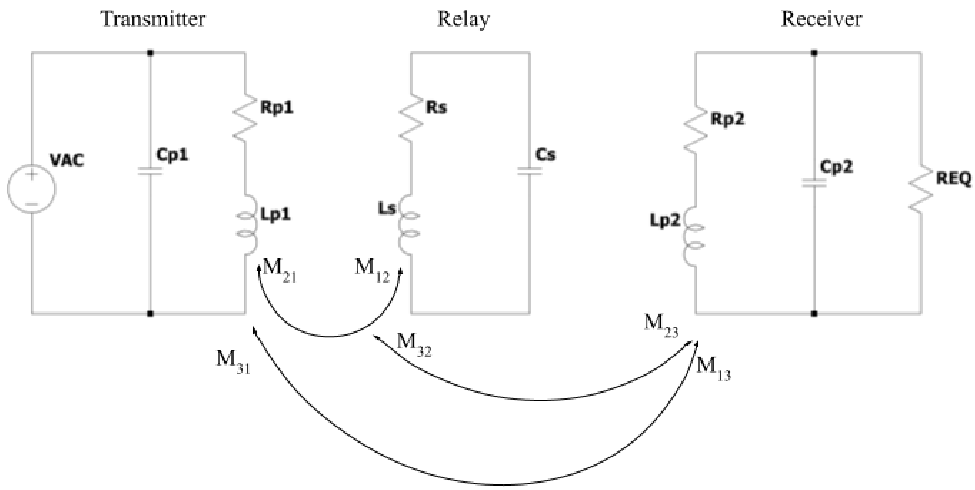

Fig. 2: The Circuit Model of the WPT System in Question. The coils are modeled with both their self-inductances and their series resistances. As for the DC voltage source and the inverter, they have been replaced with an equivalent AC voltage source. The mutual inductances or "M's" are the result of coil geometries and relative positions and orientations.

$$\begin{bmatrix} V_1 \\ 0 \\ 0 \end{bmatrix} = \begin{bmatrix} R_{p1} + j\omega L_{p1} & j\omega M_{12} & j\omega M_{13} \\ j\omega M_{21} & R_s + j\left(\omega L_s - \frac{1}{\omega C_s}\right) & j\omega M_{23} \\ j\omega M_{31} & j\omega M_{32} & R_{p2} + j\omega L_{p2} + REQ \,||\, \frac{-j}{\omega C_{p2}} \end{bmatrix} \begin{bmatrix} I_1 \\ I_2 \\ I_3 \end{bmatrix} \quad (1)$$

Since this thesis uses a pre-manufactured WPT system with available datasheets, all of the parameters can be obtained easily except for the mutual inductances. These require analytical models dependent on coil geometries and orientations.

II-A1 Air-Core Mutual Inductance

From [9], the mutual inductance between two circular air-core planar coils is given by equations (2) - (7).

$$M = \rho \times \sum_{i}^{i=n_p} \sum_{j}^{j=n_s} M_{ij} \tag{2}$$

$$M_{ij} = \frac{\mu_0 \pi a_i^2 b_j^2}{2\left(a_i^2 + b_j^2 + d^2\right)^{\frac{3}{2}}} \left(1 + \frac{15}{32}\gamma_{ij}^2 + \frac{315}{1024}\gamma_{ij}^4\right) \tag{3}$$

$$a_i = r_{out_p} - (n_i - 1)(w_p + s_p) - \frac{w_p}{2} \tag{4}$$

$$b_j = r_{out_s} - (n_j - 1)(w_s + s_s) - \frac{w_s}{2} \tag{5}$$

$$\gamma_{ij} = \frac{2a_i b_j}{\left(a_i^2 + b_j^2 + d^2\right)} \tag{6}$$

$$\rho = 1 \tag{7}$$

Where the parameters are as follows,

- M is the *Total Mutual Inductance*
- M_{ij} is the *Mut. Ind. between Loop i of Primary and Loop j of Secondary*
- r_{out_p} *Outer Radius of Primary Coil*
- r_{out_s} *Outer Radius of Secondary Coil*
- n_p is the *Number of Turns in Primary Coil*
- n_s is the *Number of Turns in Secondary Coil*
- w_p is the *Width of Copper Wire in Primary Coil*
- w_s is the *Width of Copper Wire in Secondary Coil*
- s_p is the *Track Separation in Primary Coil*
- s_s is the *Track Separation in Secondary Coil*
- ρ is a *Constant Dependent on Coil Shape* (in this case circular)
- d is the *Coaxial Distance between Coils*

Note that, here, *M* can represent *any* total mutual inductance between *any* pair of primary and secondary coils. For example, ”primary” could mean the coil of the transmitter and ”secondary” could mean the coil of the relay, or vice versa, or some other combination of *different* coils.

II-A2 Ferrite-Core Mutual Inductance

Although a hollow-cylinder ferrite core is used, for analysis purposes it can be approximated as an equivalent ferrite rod with a radius smaller than that of the innermost loop of the planar coil. The reasoning behind this extends from the approach in [10] and was later confirmed by matching model data to experimental data. The transformation is done as follows,

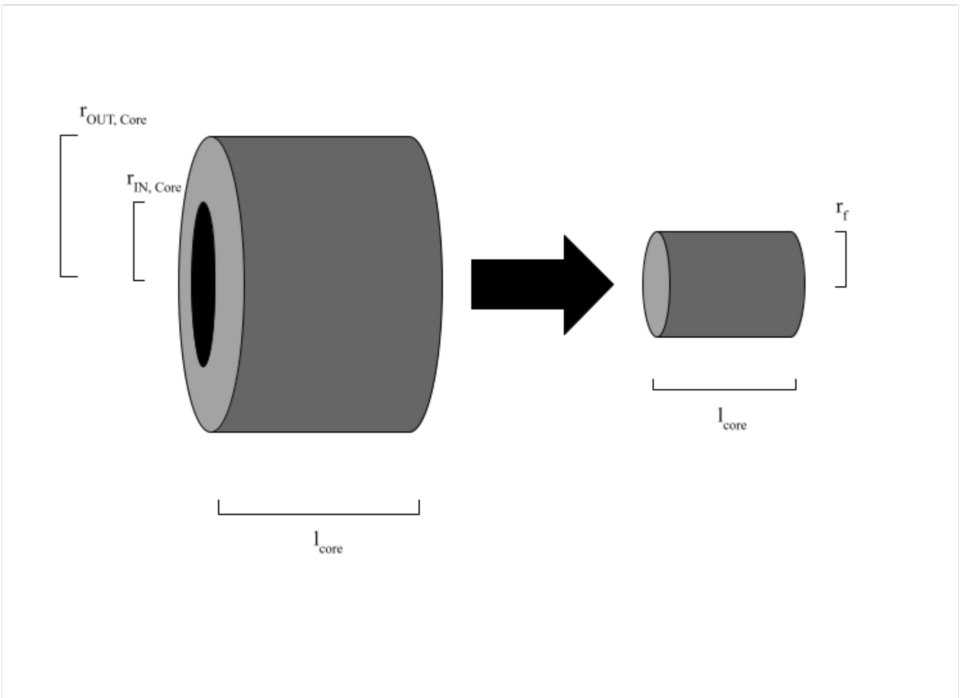

Fig. 3: The Theoretical Transformation of the Ferrite Core.

$$r_f = \left(r^2_{OUT_{Core}} - r^2_{IN_{Core}}\right)^{\frac{1}{2}} \quad (8)$$

From [11], when the average radius of the coil is larger than the radius of the core, the mutual inductance can be approximated as follows,

$$M = M_{AirCore}\left[\left[1 - \frac{r_f^2}{r_s^2}\right] + \frac{\mu_{Core_{Avg}}}{1 + D_{fc}\left(\mu_{Core_{Avg}} - 1\right)}\left[\frac{r_f^2}{r_s^2}\right]\right] \tag{9}$$

$$D_{fc} = \frac{3.966(0.5K)^{-0.056}}{|d|^3}(\frac{1}{K^2})\left[|d| - arctan\,|d|\right] \tag{10}$$

$$K = \frac{l_{core}}{r_{core}} \tag{11}$$

$$d = \left[1 - (\frac{2}{K}^2)\right]^{\frac{1}{2}} \tag{12}$$

Where the parameters are as follows,

- M is the *Total Mutual Inductance*
- $M_{AirCore}$ is the *Mut. Ind. in Calculated as Though Ferrite Core is Removed*
- $r_{In_{Core}}$ is the *Inner Radius of Hollow Ferrite Cylinder*
- $r_{Out_{Core}}$ is the *Outer Radius of Hollow Ferrite Cylinder*
- r_f is the *Equivalent Radius of Ferrite Rod*
- l_{core} is the *Length of Ferrite Core*
- r_s is the *Average Radius of Coil*
- $\mu_{Core_{Avg}}$ is the *Average Permeability of Core*
- D_{fc} is the *Demagnetization Factor*

II-B Taidacent WPT System Model and Math

With the general math model, the specific parameters of the system under test can be used to determined the theoretical output power characteristics. See Tables I and II for parameter values. For each of the distance configurations, the output power is calculated as the load is swept logarithmically from 1Ω to 1MegaΩ. See Tables III and IV for the output power characteristics. The distance configurations are as follows:

- Configuration #1: $d_{13} = 0.2$m, d_{23} determined experimentally by point of maximum voltage (see Tables III and IV)
- Configuration #2: $d_{13} = 0.4$m, d_{23} determined experimentally by point of maximum voltage (see Tables III and IV)
- Configuration #3: $d_{13} = 0.6$m, d_{23} determined experimentally by point of maximum voltage (see Tables III and IV)
- Configuration #4: $d_{13} = 0.8$m, d_{23} determined experimentally by point of maximum voltage (see Tables III and IV)
- Configuration #5: $d_{13} = 1.0$m, d_{23} determined experimentally by point of maximum voltage (see Tables III and IV)

	Configuration #1	**Configuration #2**	**Configuration #3**	**Configuration #4**	**Configuration #5**
1 Ω ($d_{23} = 0.015$m)	2660	51.9	4.36	0.72	0.174
10 Ω ($d_{23} = 0.015$m)	21100	411	34.5	5.72	1.38
100 Ω ($d_{23} = 0.02$m)	48800	917	76.5	12.6	3.09
1000 Ω ($d_{23} = 0.045$m)	82700	1120	103	17.5	4.17
10000 Ω ($d_{23} = 0.05$m)	17900	283	22.4	3.62	0.873
100000 Ω ($d_{23} = 0.05$m)	1950	30.8	2.04	0.396	0.0957
1000000 Ω ($d_{23} = 0.05$m)	197	3.11	0.205	0.0400	0.00966

TABLE III: Air-Core Model Data in [μW]

	Configuration #1	**Configuration #2**	**Configuration #3**	**Configuration #4**	**Configuration #5**
1 Ω ($d_{23} = 0.015$m)	2710	52.8	4.44	0.736	0.178
10 Ω ($d_{23} = 0.015$m)	21900	428	36.0	5.97	1.45
100 Ω ($d_{23} = 0.03$m)	52900	996	83.3	13.85	3.38
1000 Ω ($d_{23} = 0.05$m)	96300	1280	119	20.2	4.81
10000 Ω ($d_{23} = 0.05$m)	21100	331	26.0	4.20	1.01
100000 Ω ($d_{23} = 0.05$m)	2300	36.0	2.35	0.460	0.110
1000000 Ω ($d_{23} = 0.05$m)	232	3.64	0.236	0.0464	0.0111

TABLE IV: Ferrite-Core Model Data in [μW]

III Experimental Setup and Procedure

The basis of the experimental setup is the Taidacent High Power Long-Distance Wireless Power Supply Module. However, the coils still need to be mounted so that they could be easily moved along a concentric line. Therefore, the setup shown in Fig. 4 is implemented, and the individual modules and their measured values are presented in Fig. 5 - 8. In addition, the following equipment was used for the experiments:

- *Siglent 1202X-E Oscilliscope*, which is used to measure the peak-to-peak voltages of the output waveforms across the load resistances.
- *TackLife DC Power Supply*, which is used to power the transmitter.

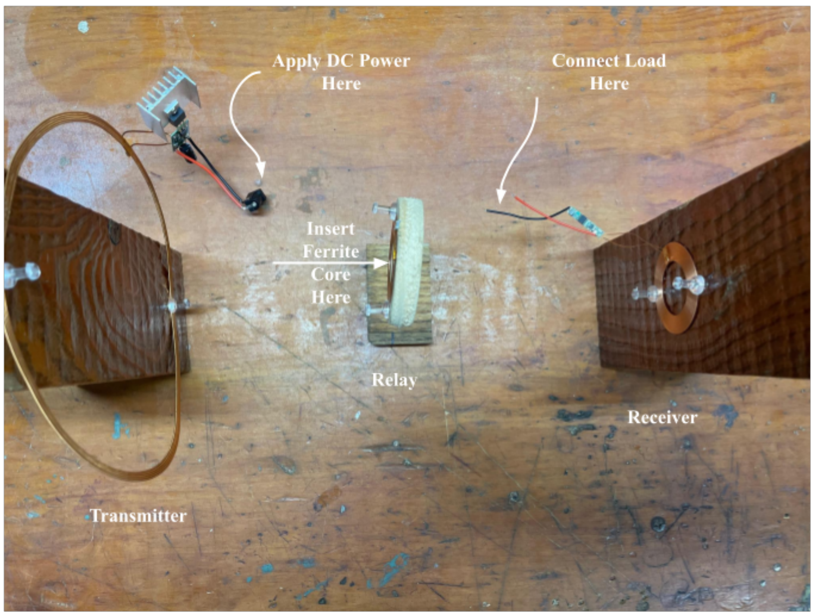

Fig. 4: The Experimental Setup of WPT System. Note that the coils are mounted such that they are all concentric, and distance between coils is changed by simply relocating a module along a coaxial line.

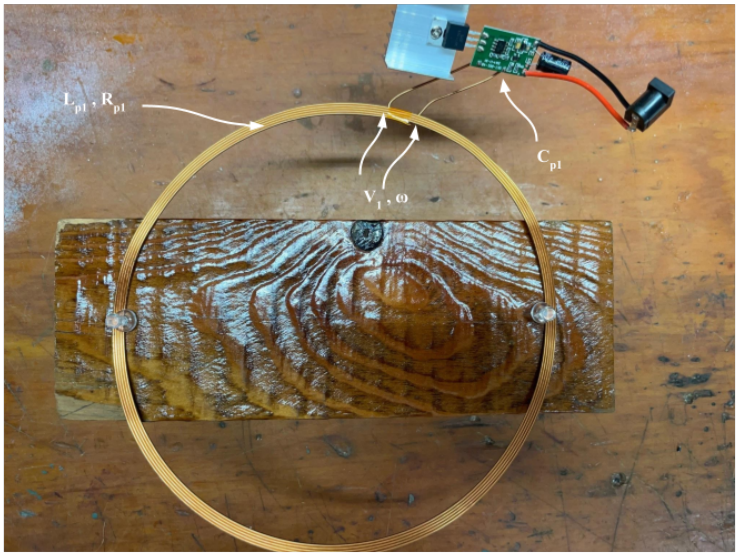

Fig. 5: The Experimental Transmitter (TX) Setup. Note that parameters indicated were measured to be $L_{p1} = 15.3\mu H$, $R_{p1} = 0.5\Omega$, $C_{p1} = 20.7nF$.

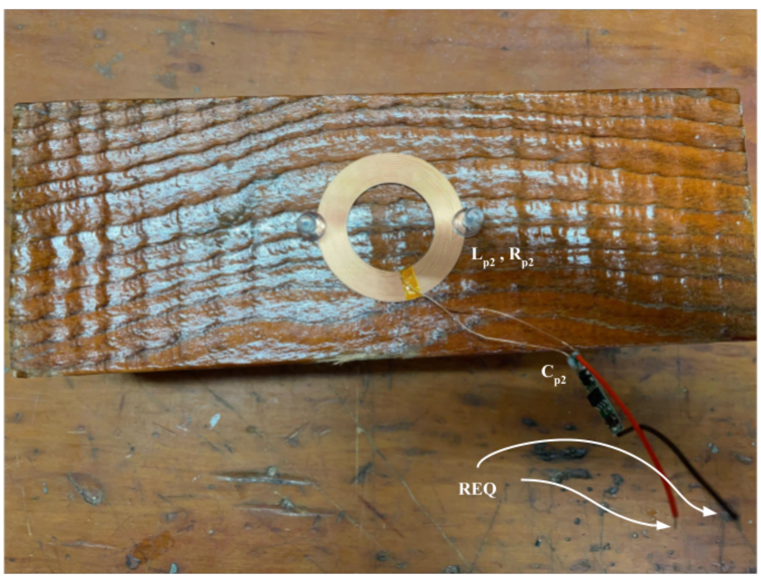

Fig. 6: The Experimental Receiver (RX) Setup. Note that parameters indicated were measured to be $L_{p2} = 50.9\mu H$, $R_{p2} = 0.9\Omega$, $C_{p2} = 15.5nF$

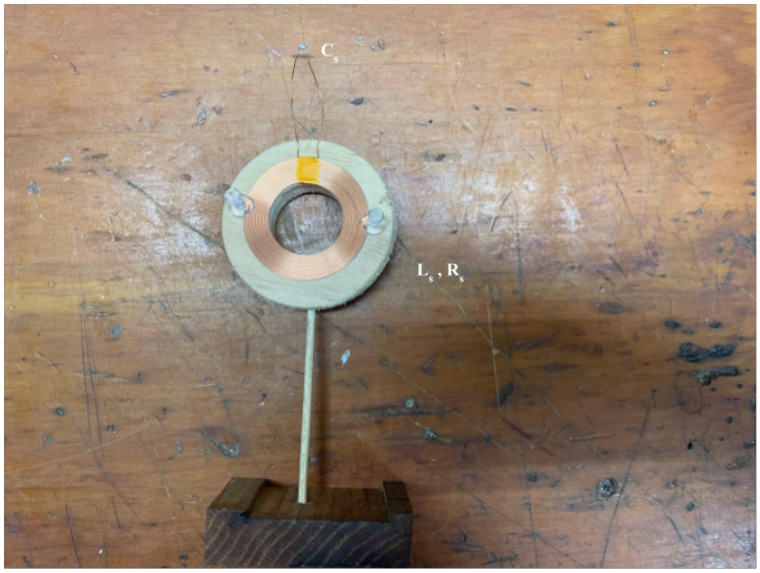

Fig. 7: The Experimental Air-Core Relay Setup. Note that parameters indicated were measured to be $L_s = 50.9\mu H$, $R_s = 0.9\Omega$, $C_s = 15.5nF$

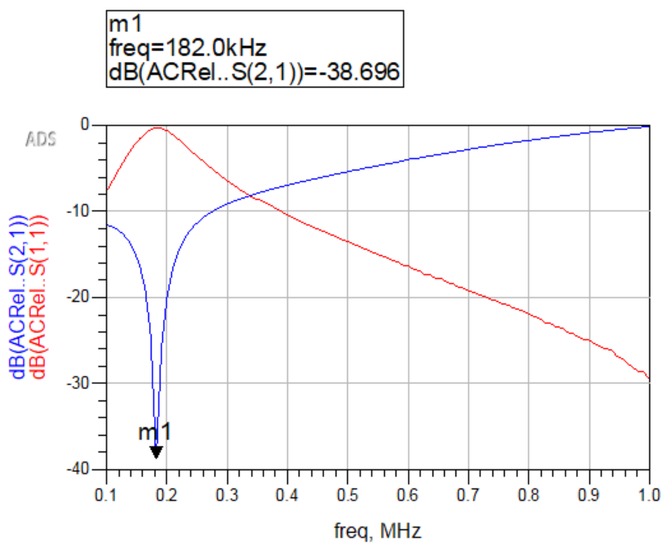

Fig. 8: The Resonance of the Experimental Air-Core Relay Setup. Note that the actual Taidacent WPT system operates at 182kHz and not 215kHz as the datasheet parameters imply.

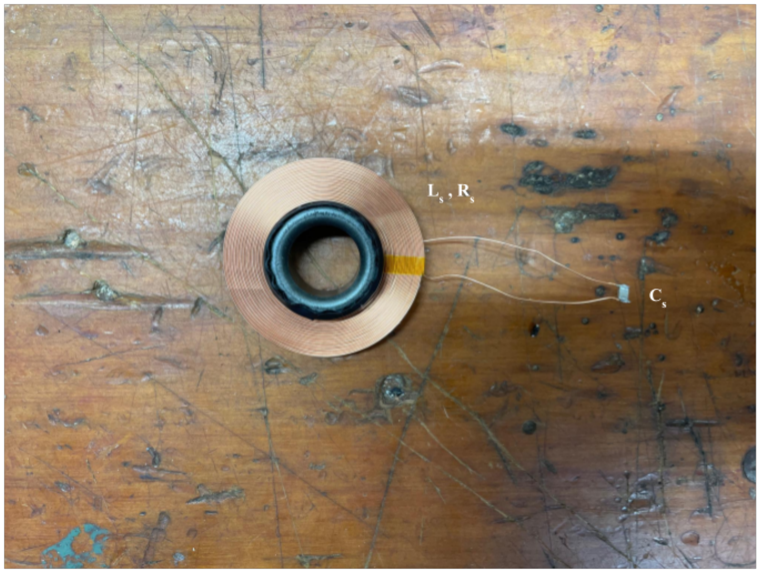

Fig. 9: The Experimental Ferrite-Core Relay Setup. Note that parameters indicated were measured to be $L_s = 75\mu H$, $R_s = 0.9\Omega$, $C_s = 10.4nF$

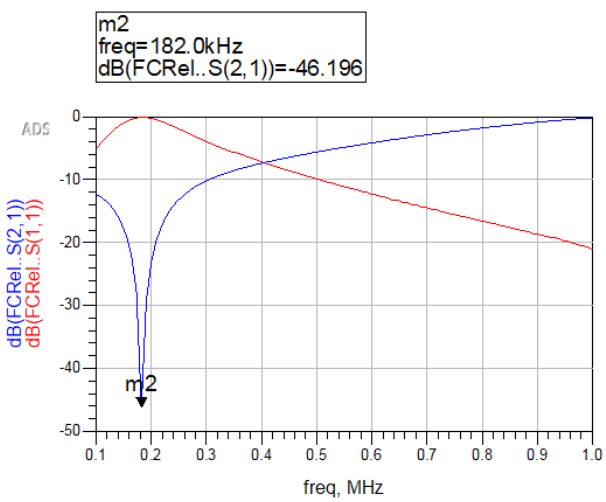

Fig. 10: The Resonance of the Experimental Ferrite-Core Relay Setup. Note that the actual Taidacent WPT system operates at 182kHz and not 215kHz as the datasheet parameters imply.

III-A Experimental Procedure

The procedure for the experiments goes as follows:

- For both air-core and ferrite-core systems,
  - Start by setting TX and RX 20cm apart and concentric.
  - Set the relay concentrically between TX and RX.
  - For each load,
    - ∗ Measure the output voltage and determine the optimal position of the relay coil between the receiver and transmitter for maximum output voltage.
    - ∗ Record voltage and calculate output power.
  - Repeat for distances of 40cm, 60cm, 80cm, and 100cm.

III-B Experimental Data

	Configuration #1	Configuration #2	Configuration #3	Configuration #4	Configuration #5
1 Ω ($d_{23} = 0.015$**m**)	2110	91.1	78.1	50	50
10 Ω ($d_{23} = 0.015$**m**)	3380	101	15.3	7.20	5
100 Ω ($d_{23} = 0.02$**m**)	19000	392	36.1	9.03	3.12
1000 Ω ($d_{23} = 0.04$**m**)	56100	994	74.1	13.6	4.05
10000 Ω ($d_{23} = 0.05$**m**)	27600	492	36.1	6.12	1.62
100000 Ω ($d_{23} = 0.05$**m**)	3590	63	4.80	0.882	0.22
1000000 Ω ($d_{23} = 0.05$**m**)	364	6.48	0.5	0.0903	0.0231

TABLE V: Experimental Air-Core Data in [μW]

	Configuration #1	Configuration #2	Configuration #3	Configuration #4	Configuration #5
1 Ω ($d_{23} = 0.015$**m**)	4510	112	12.5	72.0	50
10 Ω ($d_{23} = 0.015$**m**)	6120	151	5.00	7.20	5
100 Ω ($d_{23} = 0.03$**m**)	40600	648	60.5	12.5	3.8
1000 Ω ($d_{23} = 0.05$**m**)	123000	1710	151	24.2	6.6
10000 Ω ($d_{23} = 0.05$**m**)	64800	1080	81.9	15.1	3.5
100000 Ω ($d_{23} = 0.05$**m**)	9240	140	11.2	1.95	0.47
1000000 Ω ($d_{23} = 0.05$**m**)	946	15.1	1.12	0.198	0.048

TABLE VI: Experimental Ferrite-Core Data in [μW]

IV Results

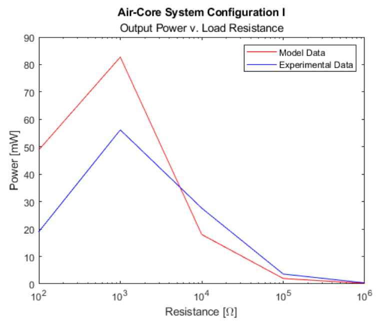

(a)

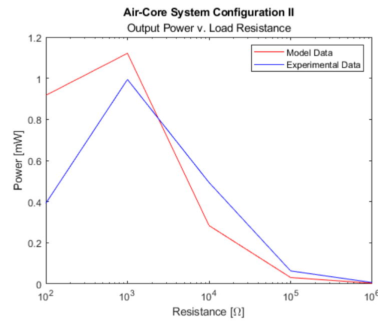

(b)

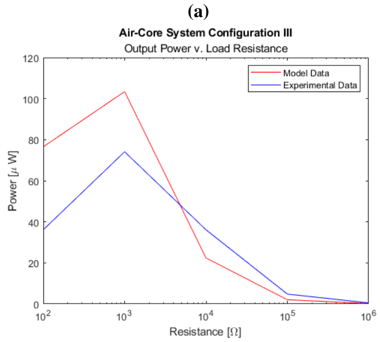

(c)

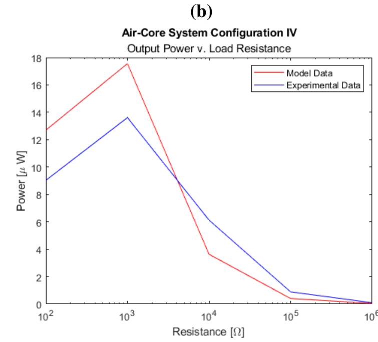

(d)

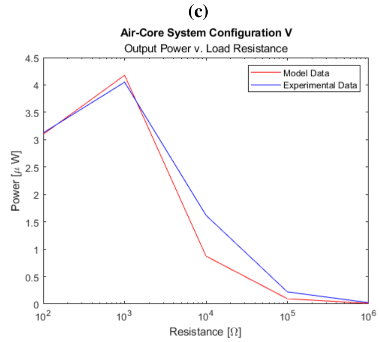

(e)

Fig. 11: Output Power Characteristics of the Air-Core-Relay WPT System

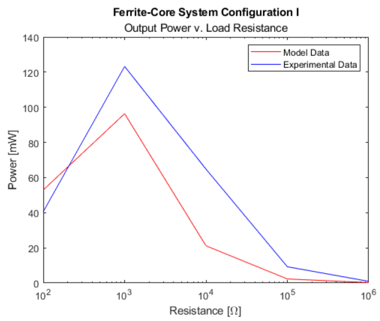

(a)

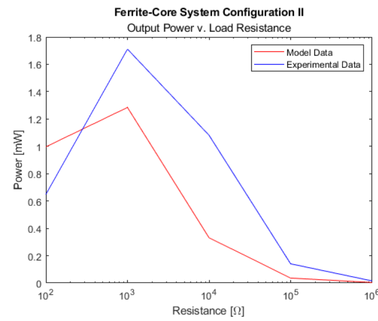

(b)

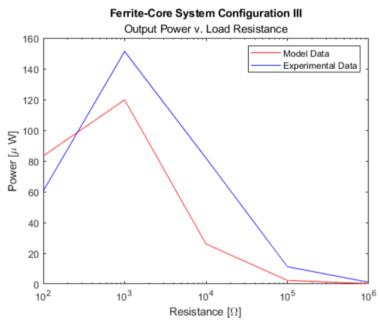

(c)

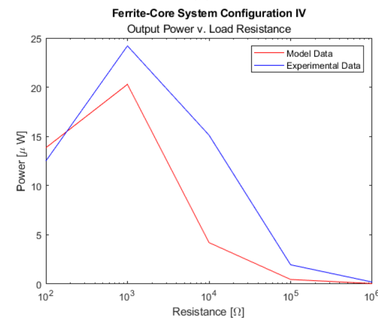

(d)

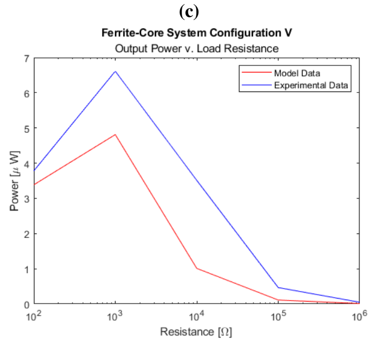

(e)

Fig. 12: Output Power Characteristics of the Ferrite-Core-Relay WPT System

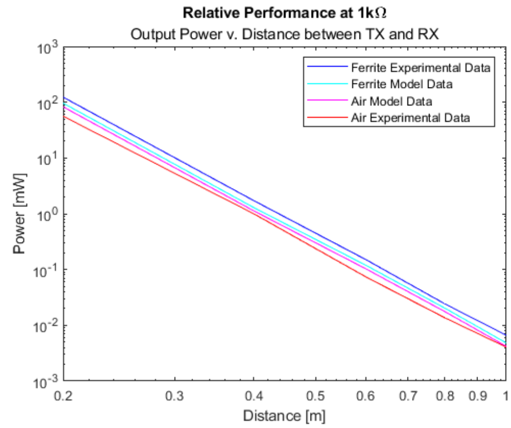

Fig. 13: The Relative Performance of Air-Core and Ferrite-Core at 1kΩ

V Discussion and Conclusion

V-A Comparison of Model and Experiment

Overall, it may be concluded from Fig. 11 and Fig. 12 that the mathematical model employed in this thesis adequately approximates the output power characteristics of both air-core-relay and ferrite-core-relay WPT systems. In the case of the air-core-relay system, the theoretical maximum output power is larger than that measured for each distance configuration. This is most probably due to inaccurate model estimates of circuit resistances. Furthermore, as the transmission distance increases, low-resistance loads yield output powers that are below the noise floor of the oscilloscope, so the measurements are inaccurate at these points. As a result, data for 1Ω and 10Ω loads are omitted in Fig. 11 and Fig. 12. Overall, the model error for each load averaged over all distance configurations is as follows,

1Ω	10Ω	100Ω	1000Ω	10000Ω	100000Ω	1000000Ω
-7427.6 %	-14.3 %	39.8 %	19.5 %	-68.6 %	-115.1 %	-120.1 %

TABLE VII: Air-Core Model Error for Each Load, Averaged Over All Distance Configurations.

In the case of the ferrite-core system, the theoretical maximum output power is generally smaller than that measured, which is probably due to the fact that the model does not accurately represent the increase in mutual inductance due to flux concentration in the ferrite core. After all, the model used in this thesis is technically not the full model developed in [11], where equation (10) presented in this paper would contain an extra term $\left(\frac{{l_{Core}}^2}{w_{Rel.}^2}\right)^{\frac{1}{3}}$ to account for the increase in flux density within the relay coil due to a long ferrite core. Again, as the transmission distance increases, low-resistance loads yield power outputs that are below the noise floor of the oscilloscope, so the measurements are inaccurate at these points. As a result, data for 1Ω and 10Ω loads are omitted in Fig. 11 and Fig. 12. Overall, the average error for each load was as follows,

1Ω	10Ω	100Ω	1000Ω	10000Ω	100000Ω	1000000Ω
-7582.8 %	-8.5 %	16.7 %	-28.8 %	-230.9 %	-322.8 %	-331.1 %

TABLE VIII: Ferrite-Core Model Error for Each Load, Averaged Over All Distance Configurations.

V-B Comparison of Systems

Upon comparing Fig. 11 and Fig. 12, the ultimate conclusion is that the addition of a ferrite core noticeably improves the output power for a given load and distance configuration. Overall, the average improvement to output power for each load as a result of using a ferrite core instead of an air core is as follows,

1Ω	10Ω	100Ω	1000Ω	10000Ω	100000Ω	1000000Ω
20%	10%	60%	90%	130%	130%	130%

TABLE IX: Percent Increase in Output Power When Switching from Air-Core Relay to Ferrite-Core Relay for Each Load, Averaged Over All Distance Configurations. Note that the apparent improvement at 1Ω and 10Ω loads is inaccurate due to noise floor issues.

The results shown in Table IX corroborate the theory embedded in equation (1). For intuition, assume the following ultra-simplified math model,

$$\begin{bmatrix} V_1 \\ 0 \\ 0 \end{bmatrix} = \begin{bmatrix} j\omega L_{p1} & 0 & 0 \\ j\omega M_{21} & 0 & 0 \\ 0 & j\omega M_{32} & j\omega L_{p2} + REQ \,||\, \frac{-j}{\omega C_{p2}} \end{bmatrix} \begin{bmatrix} I_1 \\ I_2 \\ I_3 \end{bmatrix} \tag{13}$$

Where the following simplifications have been made:

- Inductor series resistances R_{p1}, R_s, and R_{p2} are approximated as zero since inductors are nearly perfect DC short circuits.
- The effects of $I_2 \times j\omega M_{12}$, $I_3 \times j\omega M_{13}$, $I_3 \times j\omega M_{23}$ and $I_1 \times j\omega M_{31}$ are approximated as zero because very low inductive coupling is assumed.

Then, the current in the inductor of the receiver can be modeled as,

$$I_3 = \frac{\frac{V_1 M_{21}}{L_{p1}} - j\omega M_{32} I_2}{j\omega L_{p2} + REQ \,||\, \frac{-j}{\omega C_{p2}}} \tag{14}$$

Now, both M_{21} and M_{32} are multiplied by a factor, k (see equation (9)), when a ferrite core is introduced. Since this is a common factor, I_3 is roughly proportional to the change in mutual inductance caused by the ferrite core. Additionally, since power is proportional to the square of the current, the power is roughly proportional to the square of the change in mutual inductance.

Also, from Table IX, we can note that the improvement to output power is more pronounced at higher resistances. However, as seen in Fig. 11 and Fig. 12, maximum power transfer for both air-core and ferrite-core systems occurs at around 1000Ω. Therefore, there must be a compromise between power output improvement and the size of the resistive load.

From Fig. 13, we can see that, assuming optimal positioning of the relay and constant load, the relationship between output power (P) and the distance between transmitter and receiver (D) is of the following forms:

$$P = kD^n \tag{15}$$

$$logP = logk + nlogD \tag{16}$$

Furthermore, we can determine the value of k and n graphically, yielding the following equations for the air-core-relay system and the ferrite-core relay system at 1000Ω,

$$P_{AirCore} = (4.1 \times 10^{-6})D^{-5.9}W \tag{17}$$

$$P_{FerriteCore} = (6.6 \times 10^{-6})D^{-6.1}W \tag{18}$$

V-C Future of Research

These facts open up many opportunities for further investigation. Future experiments could attempt to directly power an actual wearable device such as a low-power remote sensor. Furthermore, experiments on the addition of ferrite cores to the TX coil and the RX coil could also be performed to see if power output characteristics are further improved.

VI Appendix: Datasheets

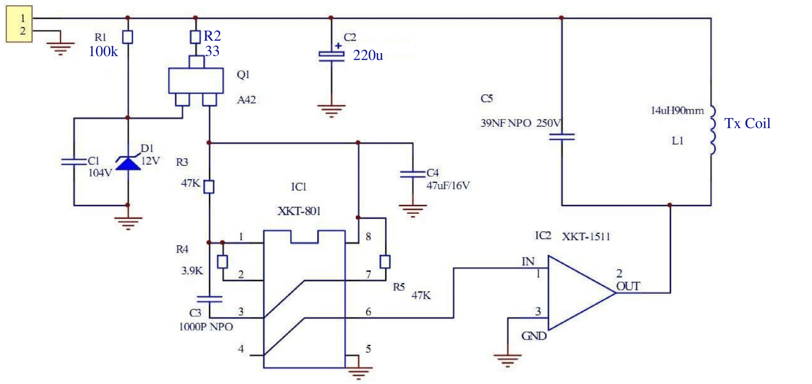

Fig. 14: Datasheet for the Taidacent Transmitter

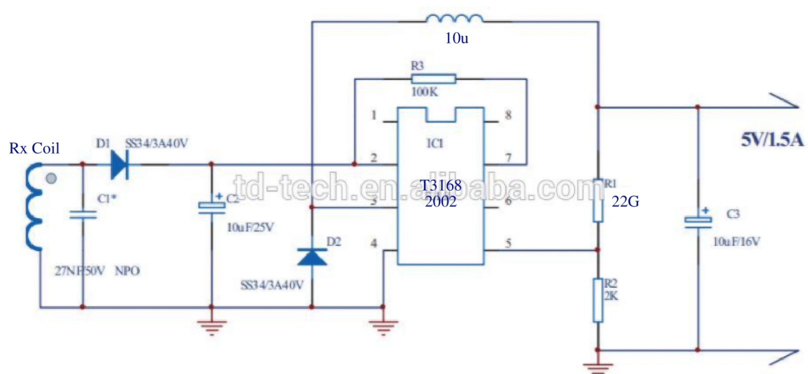

Fig. 15: Datasheet for the Taidacent Receiver. Note that the only part used in this thesis is the "Rx Coil" in parallel with "C1*". The diode "D1" is desoldered and so LC circuit is disconnected from the rest of the circuit.

VII Appendix: MATLAB Code

```
%% HON-403: Thesis Math
% Title: The Effect of a Ferrite-Core Relay on the Ouput Power
% Characteristics of a Three-Coil WPT System
% Author: Jakob White
% Date: Jul. 24, 2021
% Description: This code is used to calculate the ouput power
% characteristics of a two different three-coil WPT systems, one with an
% air-core relay and one with a ferrite-core relay. First, mutual
% inductances are calculated. Next, inductor currents are calculated.
% Then, voltages across the load resistors are calculated. Finally, output
% powers are calculated.

%% Experimental Results: Air Core

clear
clc
close all

REQ = [1 10 100 1000 10000 100000 1000000]; %Ohms

Air_Core_Config_1_Voltages = [0.13 0.52 3.9 21.2 47 53.6 54]/2;
Air_Core_Config_2_Voltages = [0.027 0.09 0.56 2.82 6.28 7.1 7.2]/2;
Air_Core_Config_3_Voltages = [0.025 0.035 0.17 0.77 1.7 1.96 2]/2;
Air_Core_Config_4_Voltages = [0.02 0.024 0.085 0.33 0.7 0.84 0.85]/2;
Air_Core_Config_5_Voltages = [0.02 0.02 0.05 0.18 0.36 0.42 0.43]/2;

Air_Core_Config_1_Powers = (((Air_Core_Config_1_Voltages).^2) ./ (2*REQ))';
Air_Core_Config_2_Powers = (((Air_Core_Config_2_Voltages).^2) ./ (2*REQ))';
Air_Core_Config_3_Powers = (((Air_Core_Config_3_Voltages).^2) ./ (2*REQ))';
```

```
Air_Core_Config_4_Powers = (((Air_Core_Config_4_Voltages).^2) ./ (2*REQ))';
Air_Core_Config_5_Powers = (((Air_Core_Config_5_Voltages).^2) ./ (2*REQ))';

%% Experimental Results: Ferrite Core
Ferrite_Core_Config_1_Voltages = [0.19 0.7 5.7 31.4 72 86 87]/2;
Ferrite_Core_Config_2_Voltages = [0.03 0.11 0.72 3.7 9.3 10.6 11]/2;
Ferrite_Core_Config_3_Voltages = [0.01 0.02 0.22 1.1 2.56 3 3]/2;
Ferrite_Core_Config_4_Voltages = [0.024 0.024 0.1 0.44 1.1 1.25 1.26]/2;
Ferrite_Core_Config_5_Voltages = [0.02 0.02 0.055 0.23 0.53 0.61 0.62]/2;

Ferrite_Core_Config_1_Powers = (((Ferrite_Core_Config_1_Voltages).^2) ./ (2*REQ))';
Ferrite_Core_Config_2_Powers = (((Ferrite_Core_Config_2_Voltages).^2) ./ (2*REQ))';
Ferrite_Core_Config_3_Powers = (((Ferrite_Core_Config_3_Voltages).^2) ./ (2*REQ))';
Ferrite_Core_Config_4_Powers = (((Ferrite_Core_Config_4_Voltages).^2) ./ (2*REQ))';
Ferrite_Core_Config_5_Powers = (((Ferrite_Core_Config_5_Voltages).^2) ./ (2*REQ))';

Power_Imp_1 = Ferrite_Core_Config_1_Powers ./ Air_Core_Config_1_Powers;
Power_Imp_2 = Ferrite_Core_Config_2_Powers ./ Air_Core_Config_2_Powers;
Power_Imp_3 = Ferrite_Core_Config_3_Powers ./ Air_Core_Config_3_Powers;
Power_Imp_4 = Ferrite_Core_Config_4_Powers ./ Air_Core_Config_4_Powers;
Power_Imp_5 = Ferrite_Core_Config_5_Powers ./ Air_Core_Config_5_Powers;

Avg_Power_Imp = (Power_Imp_1 + Power_Imp_2 + Power_Imp_3 + Power_Imp_4 + Power_Imp_5) / 5;

%% Experimental Results: Two-Coil System

Two_Coil_Config_1_Voltages = [0.07 0.2 1.38 9.36 16.2 17.4 17.4]/2;
Two_Coil_Config_2_Voltages = [0.02 0.04 0.21 1.3 2.4 2.5 2.5]/2;
```

```
Two_Coil_Config_3_Voltages = [0.02 0.02 0.07 0.4 0.7 0.75 0.76]/2;
Two_Coil_Config_4_Voltages = [0.02 0.03 0.04 0.18 0.31 0.32 0.33]/2;
Two_Coil_Config_5_Voltages = [0.02 0.02 0.04 0.1 0.17 0.18 0.18]/2;

Two_Coil_Config_1_Powers = ((Two_Coil_Config_1_Voltages).^2) ./ (2*REQ);
Two_Coil_Config_2_Powers = ((Two_Coil_Config_2_Voltages).^2) ./ (2*REQ);
Two_Coil_Config_3_Powers = ((Two_Coil_Config_3_Voltages).^2) ./ (2*REQ);
Two_Coil_Config_4_Powers = ((Two_Coil_Config_4_Voltages).^2) ./ (2*REQ);
Two_Coil_Config_5_Powers = ((Two_Coil_Config_5_Voltages).^2) ./ (2*REQ);

%% Air Core Experiments: Mutual Inductances

%Distances between TX Coil and Relay Coil in 5 Different Configurations
D12_Air_Core_1 = [18.5 18.5 18 15.5 15 15 15]/100; %m
D12_Air_Core_2 = [38.5 38.5 38 36 35 35 35]/100; %m
D12_Air_Core_3 = [58.5 58.5 58 55.5 55 55.5 55.5]/100; %m
D12_Air_Core_4 = [78.5 78.5 78 75 75 75 75]/100; %m
D12_Air_Core_5 = [98.5 98.5 98 95 95 95 95]/100; %m

%Distances between TX Coil and Relay Coil in 5 Different Configurations
D21_Air_Core_1 = D12_Air_Core_1; %m
D21_Air_Core_2 = D12_Air_Core_2; %m
D21_Air_Core_3 = D12_Air_Core_3; %m
D21_Air_Core_4 = D12_Air_Core_4; %m
D21_Air_Core_5 = D12_Air_Core_5; %m

%Distances between TX Coil and RX Coil in 5 Different Configurations
D13_Air_Core_1 = [20 20 20 20 20 20 20]/100; %m
D13_Air_Core_2 = [40 40 40 40 40 40 40]/100; %m
D13_Air_Core_3 = [60 60 60 60 60 60 60]/100; %m
D13_Air_Core_4 = [80 80 80 80 80 80 80]/100; %m
D13_Air_Core_5 = [100 100 100 100 100 100 100]/100; %m
```

```
%Distances between TX Coil and RX Coil in 5 Different Configurations
D31_Air_Core_1 = D13_Air_Core_1; %m
D31_Air_Core_2 = D13_Air_Core_2; %m
D31_Air_Core_3 = D13_Air_Core_3; %m
D31_Air_Core_4 = D13_Air_Core_4; %m
D31_Air_Core_5 = D13_Air_Core_5; %m

%Distances between RX Coil and Relay Coil in 5 Different Configurations
D23_Air_Core_1 = D13_Air_Core_1 - D12_Air_Core_1; %m
D23_Air_Core_2 = D13_Air_Core_2 - D12_Air_Core_2; %m
D23_Air_Core_3 = D13_Air_Core_3 - D12_Air_Core_3; %m
D23_Air_Core_4 = D13_Air_Core_4 - D12_Air_Core_4; %m
D23_Air_Core_5 = D13_Air_Core_5 - D12_Air_Core_5; %m

%Distances between RX Coil and Relay Coil in 5 Different Configurations
D32_Air_Core_1 = D23_Air_Core_1; %m
D32_Air_Core_2 = D23_Air_Core_2; %m
D32_Air_Core_3 = D23_Air_Core_3; %m
D32_Air_Core_4 = D23_Air_Core_4; %m
D32_Air_Core_5 = D23_Air_Core_5; %m

%M12
mu_0 = 4*pi*10^-7; %H/m
N1 = 5;
r1 = 0.1; %m
w1 = 0.0011938; %m
N2 = 15;
r2 = 0.025; %m
w2 = 0.0004445; %m

D = [D12_Air_Core_1; D12_Air_Core_2; D12_Air_Core_3; D12_Air_Core_4;
    D12_Air_Core_5];
M = zeros(5,7);

for i = 1:5
    for q = 1:7
        for j = 1:N1
            for k = 1:N2
```

```
                a = r1 - (i - 1)*(w1) - (w1/2);
                b = r2 - (j-1)*(w2) - (w2/2);
                y = 2*a*b ./ (((a)^2)+((b)^2)+((D(i,q)).^2));
                M(i,q) = M(i,q) + ((mu_0)*(pi)*((a)^2)*((b)^2) ./
                    (2*(((a)^2)+((b)^2)+((D(i,q)).^2)).^(3/2))).*...
                (1 + (15*(y.^2)/32) + (315*(y.^4)/1024));
            end
        end
    end
end

M12_Air_Core_1 = M(1,:);
M12_Air_Core_2 = M(2,:);
M12_Air_Core_3 = M(3,:);
M12_Air_Core_4 = M(4,:);
M12_Air_Core_5 = M(5,:);

%M13
mu_0 = 4*pi*10^-7; %H/m
N1 = 5;
r1 = 0.1; %m
w1 = 0.0011938; %m
N2 = 15;
r2 = 0.025; %m
w2 = 0.0004445; %m

D = [D13_Air_Core_1; D13_Air_Core_2; D13_Air_Core_3; D13_Air_Core_4;
    D13_Air_Core_5];
M = zeros(5,7);

for i = 1:5
    for q = 1:7
        for j = 1:N1
            for k = 1:N2
                a = r1 - (i - 1)*(w1) - (w1/2);
                b = r2 - (j-1)*(w2) - (w2/2);
                y = 2*a*b ./ (((a)^2)+((b)^2)+((D(i,q)).^2));
```

```
                    M(i,q) = M(i,q) + ((mu_0)*(pi)*((a)^2)*((b)^2) ./ (2*(((a)^2)+((b)^2)+((D(i,q)).^2)).^(3/2))).*...
                    (1 + (15*(y.^2)/32) + (315*(y.^4)/1024));
                end
            end
        end
end

M13_Air_Core_1 = M(1,:);
M13_Air_Core_2 = M(2,:);
M13_Air_Core_3 = M(3,:);
M13_Air_Core_4 = M(4,:);
M13_Air_Core_5 = M(5,:);

%M21
mu_0 = 4*pi*10^-7; %H/m
N2 = 5;
r2 = 0.1; %m
w2 = 0.0011938; %m
N1 = 15;
r1 = 0.025; %m
w1 = 0.0004445; %m

D = [D21_Air_Core_1; D21_Air_Core_2; D21_Air_Core_3; D21_Air_Core_4; D21_Air_Core_5];
M = zeros(5,7);

for i = 1:5
    for q = 1:7
        for j = 1:N1
            for k = 1:N2
                a = r1 - (i - 1)*(w1) - (w1/2);
                b = r2 - (j-1)*(w2) - (w2/2);
                y = 2*a*b ./ (((a)^2)+((b)^2)+((D(i,q)).^2));
                M(i,q) = M(i,q) + ((mu_0)*(pi)*((a)^2)*((b)^2) ./ (2*(((a)^2)+((b)^2)+((D(i,q)).^2)).^(3/2))).*...
                (1 + (15*(y.^2)/32) + (315*(y.^4)/1024));
            end
```

```
            end
        end
    end

    M21_Air_Core_1 = M(1,:);
    M21_Air_Core_2 = M(2,:);
    M21_Air_Core_3 = M(3,:);
    M21_Air_Core_4 = M(4,:);
    M21_Air_Core_5 = M(5,:);

    %M23
    mu_0 = 4*pi*10^-7; %H/m
    N1 = 15;
    r1 = 0.025; %m
    w1 = 0.0004445; %m
    N2 = 15;
    r2 = 0.025; %m
    w2 = 0.0004445; %m

    D = [D23_Air_Core_1; D23_Air_Core_2; D23_Air_Core_3; D23_Air_Core_4;
        D23_Air_Core_5];
    M = zeros(5,7);

    for i = 1:5
        for q = 1:7
            for j = 1:N1
                for k = 1:N2
                    a = r1 - (i - 1)*(w1) - (w1/2);
                    b = r2 - (j-1)*(w2) - (w2/2);
                    y = 2*a*b ./ (((a)^2)+((b)^2)+((D(i,q)).^2));
                    M(i,q) = M(i,q) + ((mu_0)*(pi)*((a)^2)*((b)^2) ./
                        (2*(((a)^2)+((b)^2)+((D(i,q)).^2)).^(3/2))).*...
                    (1 + (15*(y.^2)/32) + (315*(y.^4)/1024));
                end
            end
        end
    end
```

```
M23_Air_Core_1 = M(1,:);
M23_Air_Core_2 = M(2,:);
M23_Air_Core_3 = M(3,:);
M23_Air_Core_4 = M(4,:);
M23_Air_Core_5 = M(5,:);

%M31
mu_0 = 4*pi*10^-7; %H/m
N2 = 5;
r2 = 0.1; %m
w2 = 0.0011938; %m
N1 = 15;
r1 = 0.025; %m
w1 = 0.0004445; %m

D = [D31_Air_Core_1; D31_Air_Core_2; D31_Air_Core_3; D31_Air_Core_4;
    D31_Air_Core_5];
M = zeros(5,7);

for i = 1:5
    for q = 1:7
        for j = 1:N1
            for k = 1:N2
                a = r1 - (i - 1)*(w1) - (w1/2);
                b = r2 - (j-1)*(w2) - (w2/2);
                y = 2*a*b ./ (((a)^2)+((b)^2)+((D(i,q)).^2));
                M(i,q) = M(i,q) + ((mu_0)*(pi)*((a)^2)*((b)^2) ./
                    (2*(((a)^2)+((b)^2)+((D(i,q)).^2)).^(3/2))).*...
                (1 + (15*(y.^2)/32) + (315*(y.^4)/1024));
            end
        end
    end
end

M31_Air_Core_1 = M(1,:);
M31_Air_Core_2 = M(2,:);
M31_Air_Core_3 = M(3,:);
M31_Air_Core_4 = M(4,:);
```

```
M31_Air_Core_5 = M(5,:);

%M32
mu_0 = 4*pi*10^-7; %H/m
N2 = 15;
r2 = 0.025; %m
w2 = 0.0004445; %m
N1 = 15;
r1 = 0.025; %m
w1 = 0.0004445; %m

D = [D32_Air_Core_1; D32_Air_Core_2; D32_Air_Core_3; D32_Air_Core_4;
    D32_Air_Core_5];
M = zeros(5,7);

for i = 1:5
    for q = 1:7
        for j = 1:N1
            for k = 1:N2
                a = r1 - (i - 1)*(w1) - (w1/2);
                b = r2 - (j-1)*(w2) - (w2/2);
                y = 2*a*b ./ (((a)^2)+((b)^2)+((D(i,q)).^2));
                M(i,q) = M(i,q) + ((mu_0)*(pi)*((a)^2)*((b)^2) ./
                    (2*(((a)^2)+((b)^2)+((D(i,q)).^2)).^(3/2))).*...
                (1 + (15*(y.^2)/32) + (315*(y.^4)/1024));
            end
        end
    end
end

M32_Air_Core_1 = M(1,:);
M32_Air_Core_2 = M(2,:);
M32_Air_Core_3 = M(3,:);
M32_Air_Core_4 = M(4,:);
M32_Air_Core_5 = M(5,:);

%% Ferrite Core Experiments: Mutual Inductances

```

```
mu_r = 1.38;
K = 1.03;
d = abs((1-(2/K)^2)^1/2);
F = (3.966*((0.5*K)^(-0.056))/(d^3))*((1/K)^2)*(d - atan(d));
Const = 0.36 + (0.64)*mu_r /(1 + F*(mu_r - 1));

%M12
M12_Ferrite_Core_1 = M12_Air_Core_1*Const;
M12_Ferrite_Core_2 = M12_Air_Core_2*Const;
M12_Ferrite_Core_3 = M12_Air_Core_3*Const;
M12_Ferrite_Core_4 = M12_Air_Core_4*Const;
M12_Ferrite_Core_5 = M12_Air_Core_5*Const;

%M13
M13_Ferrite_Core_1 = M13_Air_Core_1;
M13_Ferrite_Core_2 = M13_Air_Core_2;
M13_Ferrite_Core_3 = M13_Air_Core_3;
M13_Ferrite_Core_4 = M13_Air_Core_4;
M13_Ferrite_Core_5 = M13_Air_Core_5;

%M21
M21_Ferrite_Core_1 = M21_Air_Core_1*Const;
M21_Ferrite_Core_2 = M21_Air_Core_2*Const;
M21_Ferrite_Core_3 = M21_Air_Core_3*Const;
M21_Ferrite_Core_4 = M21_Air_Core_4*Const;
M21_Ferrite_Core_5 = M21_Air_Core_5*Const;

%M23
M23_Ferrite_Core_1 = M23_Air_Core_1*Const;
M23_Ferrite_Core_2 = M23_Air_Core_2*Const;
M23_Ferrite_Core_3 = M23_Air_Core_3*Const;
M23_Ferrite_Core_4 = M23_Air_Core_4*Const;
M23_Ferrite_Core_5 = M23_Air_Core_5*Const;

%M31
M31_Ferrite_Core_1 = M31_Air_Core_1;
M31_Ferrite_Core_2 = M31_Air_Core_2;
M31_Ferrite_Core_3 = M31_Air_Core_3;
```

```
M31_Ferrite_Core_4 = M31_Air_Core_4;
M31_Ferrite_Core_5 = M31_Air_Core_5;

%M32
M32_Ferrite_Core_1 = M32_Air_Core_1*Const;
M32_Ferrite_Core_2 = M32_Air_Core_2*Const;
M32_Ferrite_Core_3 = M32_Air_Core_3*Const;
M32_Ferrite_Core_4 = M32_Air_Core_4*Const;
M32_Ferrite_Core_5 = M32_Air_Core_5*Const;

%% Air Core Experiments: Output Currents

f = 215*10^3; %Hz
w = 2*pi*f;

V1 = 100; %V
V2 = 0;
V3 = 0;

Rp1 = 0.5; %Ohms
Lp1 = 14*10^-6; %Henries
Cp1 = 39*10^-9; %Farads

Rs = 0.9; %Ohm
Ls = 20*10^-6; %Henries
Cs = 27*10^-9; %Farads

Rp2 = 0.9; %Ohms
Lp2 = 20*10^-6; %Henries
Cp2 = 27*10^-9; %Farads

k12_Air_Core_1 = M12_Air_Core_1/sqrt(Lp1*Ls);
k12_Air_Core_2 = M12_Air_Core_2/sqrt(Lp1*Ls);
k12_Air_Core_3 = M12_Air_Core_3/sqrt(Lp1*Ls);
k12_Air_Core_4 = M12_Air_Core_4/sqrt(Lp1*Ls);
k12_Air_Core_5 = M12_Air_Core_5/sqrt(Lp1*Ls);

k13_Air_Core_1 = M13_Air_Core_1/sqrt(Lp1*Lp2);
```

```
k13_Air_Core_2 = M13_Air_Core_2/sqrt(Lp1*Lp2);
k13_Air_Core_3 = M13_Air_Core_3/sqrt(Lp1*Lp2);
k13_Air_Core_4 = M13_Air_Core_4/sqrt(Lp1*Lp2);
k13_Air_Core_5 = M13_Air_Core_5/sqrt(Lp1*Lp2);

k21_Air_Core_1 = M21_Air_Core_1/sqrt(Lp1*Ls);
k21_Air_Core_2 = M21_Air_Core_2/sqrt(Lp1*Ls);
k21_Air_Core_3 = M21_Air_Core_3/sqrt(Lp1*Ls);
k21_Air_Core_4 = M21_Air_Core_4/sqrt(Lp1*Ls);
k21_Air_Core_5 = M21_Air_Core_5/sqrt(Lp1*Ls);

k23_Air_Core_1 = M23_Air_Core_1/sqrt(Lp2*Ls);
k23_Air_Core_2 = M23_Air_Core_2/sqrt(Lp2*Ls);
k23_Air_Core_3 = M23_Air_Core_3/sqrt(Lp2*Ls);
k23_Air_Core_4 = M23_Air_Core_4/sqrt(Lp2*Ls);
k23_Air_Core_5 = M23_Air_Core_5/sqrt(Lp2*Ls);

k31_Air_Core_1 = M31_Air_Core_1/sqrt(Lp1*Lp2);
k31_Air_Core_2 = M31_Air_Core_2/sqrt(Lp1*Lp2);
k31_Air_Core_3 = M31_Air_Core_3/sqrt(Lp1*Lp2);
k31_Air_Core_4 = M31_Air_Core_4/sqrt(Lp1*Lp2);
k31_Air_Core_5 = M31_Air_Core_5/sqrt(Lp1*Lp2);

k32_Air_Core_1 = M32_Air_Core_1/sqrt(Lp2*Ls);
k32_Air_Core_2 = M32_Air_Core_2/sqrt(Lp2*Ls);
k32_Air_Core_3 = M32_Air_Core_3/sqrt(Lp2*Ls);
k32_Air_Core_4 = M32_Air_Core_4/sqrt(Lp2*Ls);
k32_Air_Core_5 = M32_Air_Core_5/sqrt(Lp2*Ls);

Currents_Air_Core_1 = zeros(3,3);
REQ_Currents_Air_Core_1 = zeros(7,1);
REQ_Voltages_Air_Core_1 = zeros(7,1);
REQ_Powers_Air_Core_1 =  zeros(7,1);

for j = 1:7

A = Rp1 + 1i*w*Lp1;
B = 1i*w*M12_Air_Core_1(j);
```

```
C = 1i*w*M13_Air_Core_1(j);

D = 1i*w*M21_Air_Core_1(j);
E = Rs + 1i*(w*Ls - (1/(w*Cs)));
F = 1i*w*M23_Air_Core_1(j);

G = 1i*w*M31_Air_Core_1(j);
H = 1i*w*M32_Air_Core_1(j);
I = Rp2 + 1i*w*Lp2 + (REQ(j)*(1/(1i*w*Cp2)))/((REQ(j)+(1/(1i*w*Cp2))));

syms I1 I2 I3
eqn1 = A*I1 + B*I2 + C*I3 == V1;
eqn2 = D*I1 + E*I2 + F*I3 == V2;
eqn3 = G*I1 + H*I2 + I*I3 == V3;

[A,B] = equationsToMatrix([eqn1, eqn2, eqn3], [I1, I2, I3]);

X = linsolve(A,B);

Currents_Air_Core_1(j,1) = X(1);
Currents_Air_Core_1(j,2) = X(2);
Currents_Air_Core_1(j,3) = X(3);

Z = abs((REQ(j).*(1/(1i*w*Cp2)))./((REQ(j)+(1/(1i*w*Cp2)))));

REQ_Currents_Air_Core_1(j) = abs(Currents_Air_Core_1(j,3))*Z/REQ(j);
REQ_Voltages_Air_Core_1(j) = REQ_Currents_Air_Core_1(j) * REQ(j);
REQ_Powers_Air_Core_1(j) = (REQ_Voltages_Air_Core_1(j)^2)/(2*REQ(j));

end

Currents_Air_Core_2 = zeros(3,3);
REQ_Currents_Air_Core_2 = zeros(7,1);
REQ_Voltages_Air_Core_2 = zeros(7,1);
REQ_Powers_Air_Core_2 = zeros(7,1);

for j = 1:7

```

```
A = Rp1 + 1i*w*Lp1;
B = 1i*w*M12_Air_Core_2(j);
C = 1i*w*M13_Air_Core_2(j);

D = 1i*w*M21_Air_Core_2(j);
E = Rs + 1i*(w*Ls - (1/(w*Cs)));
F = 1i*w*M23_Air_Core_2(j);

G = 1i*w*M31_Air_Core_2(j);
H = 1i*w*M32_Air_Core_2(j);
I = Rp2 + 1i*w*Lp2 + (REQ(j)*(1/(1i*w*Cp2)))/((REQ(j)+(1/(1i*w*Cp2))));

syms I1 I2 I3
eqn1 = A*I1 + B*I2 + C*I3 == V1;
eqn2 = D*I1 + E*I2 + F*I3 == V2;
eqn3 = G*I1 + H*I2 + I*I3 == V3;

[A,B] = equationsToMatrix([eqn1, eqn2, eqn3], [I1, I2, I3]);

X = linsolve(A,B);

Currents_Air_Core_2(j,1) = X(1);
Currents_Air_Core_2(j,2) = X(2);
Currents_Air_Core_2(j,3) = X(3);

Z = abs((REQ(j).*(1/(1i*w*Cp2)))./((REQ(j)+(1/(1i*w*Cp2)))));

REQ_Currents_Air_Core_2(j) = abs(Currents_Air_Core_2(j,3))*Z/REQ(j);
REQ_Voltages_Air_Core_2(j) = REQ_Currents_Air_Core_2(j) * REQ(j);
REQ_Powers_Air_Core_2(j) = (REQ_Voltages_Air_Core_2(j)^2)/(2*REQ(j));

end

Currents_Air_Core_3 = zeros(3,3);
REQ_Currents_Air_Core_3 = zeros(7,1);
REQ_Voltages_Air_Core_3 = zeros(7,1);
REQ_Powers_Air_Core_3 = zeros(7,1);
```

```
for j = 1:7

A = Rp1 + 1i*w*Lp1;
B = 1i*w*M12_Air_Core_3(j);
C = 1i*w*M13_Air_Core_3(j);

D = 1i*w*M21_Air_Core_3(j);
E = Rs + 1i*(w*Ls - (1/(w*Cs)));
F = 1i*w*M23_Air_Core_3(j);

G = 1i*w*M31_Air_Core_3(j);
H = 1i*w*M32_Air_Core_3(j);
I = Rp2 + 1i*w*Lp2 + (REQ(j)*(1/(1i*w*Cp2)))/((REQ(j)+(1/(1i*w*Cp2))));

syms I1 I2 I3
eqn1 = A*I1 + B*I2 + C*I3 == V1;
eqn2 = D*I1 + E*I2 + F*I3 == V2;
eqn3 = G*I1 + H*I2 + I*I3 == V3;

[A,B] = equationsToMatrix([eqn1, eqn2, eqn3], [I1, I2, I3]);

X = linsolve(A,B);

Currents_Air_Core_3(j,1) = X(1);
Currents_Air_Core_3(j,2) = X(2);
Currents_Air_Core_3(j,3) = X(3);

Z = abs((REQ(j).*(1/(1i*w*Cp2)))./((REQ(j)+(1/(1i*w*Cp2)))));

REQ_Currents_Air_Core_3(j) = abs(Currents_Air_Core_3(j,3))*Z/REQ(j);
REQ_Voltages_Air_Core_3(j) = REQ_Currents_Air_Core_3(j) * REQ(j);
REQ_Powers_Air_Core_3(j) = (REQ_Voltages_Air_Core_3(j)^2)/(2*REQ(j));

end

Currents_Air_Core_4 = zeros(3,3);
REQ_Currents_Air_Core_4 = zeros(7,1);
REQ_Voltages_Air_Core_4 = zeros(7,1);
```

```
REQ_Powers_Air_Core_4 = zeros(7,1);

for j = 1:7

A = Rp1 + 1i*w*Lp1;
B = 1i*w*M12_Air_Core_4(j);
C = 1i*w*M13_Air_Core_4(j);

D = 1i*w*M21_Air_Core_4(j);
E = Rs + 1i*(w*Ls - (1/(w*Cs)));
F = 1i*w*M23_Air_Core_4(j);

G = 1i*w*M31_Air_Core_4(j);
H = 1i*w*M32_Air_Core_4(j);
I = Rp2 + 1i*w*Lp2 + (REQ(j)*(1/(1i*w*Cp2)))/((REQ(j)+(1/(1i*w*Cp2))));

syms I1 I2 I3
eqn1 = A*I1 + B*I2 + C*I3 == V1;
eqn2 = D*I1 + E*I2 + F*I3 == V2;
eqn3 = G*I1 + H*I2 + I*I3 == V3;

[A,B] = equationsToMatrix([eqn1, eqn2, eqn3], [I1, I2, I3]);

X = linsolve(A,B);

Currents_Air_Core_4(j,1) = X(1);
Currents_Air_Core_4(j,2) = X(2);
Currents_Air_Core_4(j,3) = X(3);

Z = abs((REQ(j).*(1/(1i*w*Cp2)))./((REQ(j)+(1/(1i*w*Cp2)))));

REQ_Currents_Air_Core_4(j) = abs(Currents_Air_Core_4(j,3))*Z/REQ(j);
REQ_Voltages_Air_Core_4(j) = REQ_Currents_Air_Core_4(j) * REQ(j);
REQ_Powers_Air_Core_4(j) = (REQ_Voltages_Air_Core_4(j)^2)/(2*REQ(j));

end

Currents_Air_Core_5 = zeros(3,3);
```

```
REQ_Currents_Air_Core_5 = zeros(7,1);
REQ_Voltages_Air_Core_5 = zeros(7,1);
REQ_Powers_Air_Core_5 = zeros(7,1);

for j = 1:7

A = Rp1 + 1i*w*Lp1;
B = 1i*w*M12_Air_Core_5(j);
C = 1i*w*M13_Air_Core_5(j);

D = 1i*w*M21_Air_Core_5(j);
E = Rs + 1i*(w*Ls - (1/(w*Cs)));
F = 1i*w*M23_Air_Core_5(j);

G = 1i*w*M31_Air_Core_5(j);
H = 1i*w*M32_Air_Core_5(j);
I = Rp2 + 1i*w*Lp2 + (REQ(j)*(1/(1i*w*Cp2)))/((REQ(j)+(1/(1i*w*Cp2))));

syms I1 I2 I3

eqn1 = A*I1 + B*I2 + C*I3 == V1;
eqn2 = D*I1 + E*I2 + F*I3 == V2;
eqn3 = G*I1 + H*I2 + I*I3 == V3;

[A,B] = equationsToMatrix([eqn1, eqn2, eqn3], [I1, I2, I3]);

X = linsolve(A,B);

Currents_Air_Core_5(j,1) = X(1);
Currents_Air_Core_5(j,2) = X(2);
Currents_Air_Core_5(j,3) = X(3);

Z = abs((REQ(j).*(1/(1i*w*Cp2)))./((REQ(j)+(1/(1i*w*Cp2)))));

REQ_Currents_Air_Core_5(j) = abs(Currents_Air_Core_5(j,3))*Z/REQ(j);
REQ_Voltages_Air_Core_5(j) = REQ_Currents_Air_Core_5(j) * REQ(j);
REQ_Powers_Air_Core_5(j) = (REQ_Voltages_Air_Core_5(j)^2)/(2*REQ(j));

```

```
end

A = 1000*REQ_Powers_Air_Core_1;
A1 = 1000*Air_Core_Config_1_Powers;
B = 1000*REQ_Powers_Air_Core_2;
B1 = 1000*Air_Core_Config_2_Powers;
C = 1000000*REQ_Powers_Air_Core_3;
C1 = 1000000*Air_Core_Config_3_Powers;
D = 1000000*REQ_Powers_Air_Core_4;
D1 = 1000000*Air_Core_Config_4_Powers;
E = 1000000*REQ_Powers_Air_Core_5;
E1 = 1000000*Air_Core_Config_5_Powers;

figure(1)
semilogx(REQ(3:7), A(3:7),'red')
hold on
semilogx(REQ(3:7), A1(3:7),'blue')
hold off
title('Air-Core System Configuration I')
subtitle('Output Power v. Load Resistance')
xlabel('Resistance [\Omega]')
ylabel('Power [mW]')
legend('Model Data','Experimental Data', 'Location', 'northeast')

figure(2)
semilogx(REQ(3:7), B(3:7),'red')
hold on
semilogx(REQ(3:7), B1(3:7),'blue')
hold off
title('Air-Core System Configuration II')
subtitle('Output Power v. Load Resistance')
xlabel('Resistance [\Omega]')
ylabel('Power [mW]')
legend('Model Data','Experimental Data', 'Location', 'northeast')

figure(3)
semilogx(REQ(3:7), C(3:7),'red')
hold on
```

```
semilogx(REQ(3:7), C1(3:7),'blue')
hold off
title('Air-Core System Configuration III')
subtitle('Output Power v. Load Resistance')
xlabel('Resistance [\Omega]')
ylabel('Power [\mu W]')
legend('Model Data','Experimental Data', 'Location', 'northeast')

figure(4)
semilogx(REQ(3:7), D(3:7),'red')
hold on
semilogx(REQ(3:7), D1(3:7),'blue')
hold off
title('Air-Core System Configuration IV')
subtitle('Output Power v. Load Resistance')
xlabel('Resistance [\Omega]')
ylabel('Power [\mu W]')
legend('Model Data','Experimental Data', 'Location', 'northeast')

figure(5)
semilogx(REQ(3:7), E(3:7),'red')
hold on
semilogx(REQ(3:7), E1(3:7),'blue')
hold off
title('Air-Core System Configuration V')
subtitle('Output Power v. Load Resistance')
xlabel('Resistance [\Omega]')
ylabel('Power [\mu W]')
legend('Model Data','Experimental Data', 'Location', 'northeast')

%% %% Ferrite Core Experiments: Output Currents

f = 215*10^3; %Hz
w = 2*pi*f;

V1 = 100; %V
V2 = 0;
V3 = 0;
```

```
Rp1 = 0.5; %Ohms
Lp1 = 14*10^-6; %Henries
Cp1 = 39*10^-9; %Farads

Rs = 0.9; %Ohm
Ls = 27*10^-6; %Henries
Cs = 20*10^-9; %Farads

Rp2 = 0.9; %Ohms
Lp2 = 20*10^-6; %Henries
Cp2 = 27*10^-9; %Farads

REQ = [1 10 100 1000 10000 100000 1000000]; %Ohms

k12_Ferrite_Core_1 = M12_Ferrite_Core_1/sqrt(Lp1*Ls);
k12_Ferrite_Core_2 = M12_Ferrite_Core_2/sqrt(Lp1*Ls);
k12_Ferrite_Core_3 = M12_Ferrite_Core_3/sqrt(Lp1*Ls);
k12_Ferrite_Core_4 = M12_Ferrite_Core_4/sqrt(Lp1*Ls);
k12_Ferrite_Core_5 = M12_Ferrite_Core_5/sqrt(Lp1*Ls);

k13_Ferrite_Core_1 = M13_Ferrite_Core_1/sqrt(Lp1*Lp2);
k13_Ferrite_Core_2 = M13_Ferrite_Core_2/sqrt(Lp1*Lp2);
k13_Ferrite_Core_3 = M13_Ferrite_Core_3/sqrt(Lp1*Lp2);
k13_Ferrite_Core_4 = M13_Ferrite_Core_4/sqrt(Lp1*Lp2);
k13_Ferrite_Core_5 = M13_Ferrite_Core_5/sqrt(Lp1*Lp2);

k21_Ferrite_Core_1 = M21_Ferrite_Core_1/sqrt(Lp1*Ls);
k21_Ferrite_Core_2 = M21_Ferrite_Core_2/sqrt(Lp1*Ls);
k21_Ferrite_Core_3 = M21_Ferrite_Core_3/sqrt(Lp1*Ls);
k21_Ferrite_Core_4 = M21_Ferrite_Core_4/sqrt(Lp1*Ls);
k21_Ferrite_Core_5 = M21_Ferrite_Core_5/sqrt(Lp1*Ls);

k23_Ferrite_Core_1 = M23_Ferrite_Core_1/sqrt(Lp2*Ls);
k23_Ferrite_Core_2 = M23_Ferrite_Core_2/sqrt(Lp2*Ls);
k23_Ferrite_Core_3 = M23_Ferrite_Core_3/sqrt(Lp2*Ls);
k23_Ferrite_Core_4 = M23_Ferrite_Core_4/sqrt(Lp2*Ls);
k23_Ferrite_Core_5 = M23_Ferrite_Core_5/sqrt(Lp2*Ls);
```

```
k31_Ferrite_Core_1 = M31_Ferrite_Core_1/sqrt(Lp1*Lp2);
k31_Ferrite_Core_2 = M31_Ferrite_Core_2/sqrt(Lp1*Lp2);
k31_Ferrite_Core_3 = M31_Ferrite_Core_3/sqrt(Lp1*Lp2);
k31_Ferrite_Core_4 = M31_Ferrite_Core_4/sqrt(Lp1*Lp2);
k31_Ferrite_Core_5 = M31_Ferrite_Core_5/sqrt(Lp1*Lp2);

k32_Ferrite_Core_1 = M32_Ferrite_Core_1/sqrt(Lp2*Ls);
k32_Ferrite_Core_2 = M32_Ferrite_Core_2/sqrt(Lp2*Ls);
k32_Ferrite_Core_3 = M32_Ferrite_Core_3/sqrt(Lp2*Ls);
k32_Ferrite_Core_4 = M32_Ferrite_Core_4/sqrt(Lp2*Ls);
k32_Ferrite_Core_5 = M32_Ferrite_Core_5/sqrt(Lp2*Ls);

Currents_Ferrite_Core_1 = zeros(3,3);
REQ_Currents_Ferrite_Core_1 = zeros(7,1);
REQ_Voltages_Ferrite_Core_1 = zeros(7,1);
REQ_Powers_Ferrite_Core_1 = zeros(7,1);

for j = 1:7

A = Rp1 + 1i*w*Lp1;
B = 1i*w*M12_Ferrite_Core_1(j);
C = 1i*w*M13_Ferrite_Core_1(j);

D = 1i*w*M21_Ferrite_Core_1(j);
E = Rs + 1i*(w*Ls - (1/(w*Cs)));
F = 1i*w*M23_Ferrite_Core_1(j);

G = 1i*w*M31_Ferrite_Core_1(j);
H = 1i*w*M32_Ferrite_Core_1(j);
I = Rp2 + 1i*w*Lp2 + (REQ(j)*(1/(1i*w*Cp2)))/((REQ(j)+(1/(1i*w*Cp2))));

syms I1 I2 I3
eqn1 = A*I1 + B*I2 + C*I3 == V1;
eqn2 = D*I1 + E*I2 + F*I3 == V2;
eqn3 = G*I1 + H*I2 + I*I3 == V3;

[A,B] = equationsToMatrix([eqn1, eqn2, eqn3], [I1, I2, I3]);
```

```
X = linsolve(A,B);

 Currents_Ferrite_Core_1(j,1) = X(1);
 Currents_Ferrite_Core_1(j,2) = X(2);
 Currents_Ferrite_Core_1(j,3) = X(3);

Z = abs((REQ(j).*(1/(1i*w*Cp2)))./((REQ(j)+(1/(1i*w*Cp2)))));

 REQ_Currents_Ferrite_Core_1(j) = abs(Currents_Ferrite_Core_1(j,3))*Z/
    REQ(j);
 REQ_Voltages_Ferrite_Core_1(j) = REQ_Currents_Ferrite_Core_1(j) * REQ(j
    );
 REQ_Powers_Ferrite_Core_1(j) = (REQ_Voltages_Ferrite_Core_1(j)^2)/(2*
    REQ(j));

 end

 Currents_Ferrite_Core_2 = zeros(3,3);
 REQ_Currents_Ferrite_Core_2 = zeros(7,1);
 REQ_Voltages_Ferrite_Core_2 = zeros(7,1);
 REQ_Powers_Ferrite_Core_2 = zeros(7,1);

 for j = 1:7

A = Rp1 + 1i*w*Lp1;
B = 1i*w*M12_Ferrite_Core_2(j);
C = 1i*w*M13_Ferrite_Core_2(j);

D = 1i*w*M21_Ferrite_Core_2(j);
E = Rs + 1i*(w*Ls - (1/(w*Cs)));
F = 1i*w*M23_Ferrite_Core_2(j);

G = 1i*w*M31_Ferrite_Core_2(j);
H = 1i*w*M32_Ferrite_Core_2(j);
I = Rp2 + 1i*w*Lp2 + (REQ(j)*(1/(1i*w*Cp2)))/((REQ(j)+(1/(1i*w*Cp2))));

syms I1 I2 I3
```

```
eqn1 = A*I1 + B*I2 + C*I3 == V1;
eqn2 = D*I1 + E*I2 + F*I3 == V2;
eqn3 = G*I1 + H*I2 + I*I3 == V3;

[A,B] = equationsToMatrix([eqn1, eqn2, eqn3], [I1, I2, I3]);

X = linsolve(A,B);

Currents_Ferrite_Core_2(j,1) = X(1);
Currents_Ferrite_Core_2(j,2) = X(2);
Currents_Ferrite_Core_2(j,3) = X(3);

Z = abs((REQ(j).*(1/(1i*w*Cp2)))./((REQ(j)+(1/(1i*w*Cp2)))));

REQ_Currents_Ferrite_Core_2(j) = abs(Currents_Ferrite_Core_2(j,3))*Z/
    REQ(j);
REQ_Voltages_Ferrite_Core_2(j) = REQ_Currents_Ferrite_Core_2(j) * REQ(j
    );
REQ_Powers_Ferrite_Core_2(j) = (REQ_Voltages_Ferrite_Core_2(j)^2)/(2*
    REQ(j));

end

Currents_Ferrite_Core_3 = zeros(3,3);
REQ_Currents_Ferrite_Core_3 = zeros(7,1);
REQ_Voltages_Ferrite_Core_3 = zeros(7,1);
REQ_Powers_Ferrite_Core_3 = zeros(7,1);

for j = 1:7

A = Rp1 + 1i*w*Lp1;
B = 1i*w*M12_Ferrite_Core_3(j);
C = 1i*w*M13_Ferrite_Core_3(j);

D = 1i*w*M21_Ferrite_Core_3(j);
E = Rs + 1i*(w*Ls - (1/(w*Cs)));
F = 1i*w*M23_Ferrite_Core_3(j);

```

```
G = 1i*w*M31_Ferrite_Core_3(j);
H = 1i*w*M32_Ferrite_Core_3(j);
I = Rp2 + 1i*w*Lp2 + (REQ(j)*(1/(1i*w*Cp2)))/((REQ(j)+(1/(1i*w*Cp2))));

syms I1 I2 I3
eqn1 = A*I1 + B*I2 + C*I3 == V1;
eqn2 = D*I1 + E*I2 + F*I3 == V2;
eqn3 = G*I1 + H*I2 + I*I3 == V3;

[A,B] = equationsToMatrix([eqn1, eqn2, eqn3], [I1, I2, I3]);

X = linsolve(A,B);

Currents_Ferrite_Core_3(j,1) = X(1);
Currents_Ferrite_Core_3(j,2) = X(2);
Currents_Ferrite_Core_3(j,3) = X(3);

Z = abs((REQ(j).*(1/(1i*w*Cp2)))./((REQ(j)+(1/(1i*w*Cp2)))));

REQ_Currents_Ferrite_Core_3(j) = abs(Currents_Ferrite_Core_3(j,3))*Z/
    REQ(j);
REQ_Voltages_Ferrite_Core_3(j) = REQ_Currents_Ferrite_Core_3(j) * REQ(j
    );
REQ_Powers_Ferrite_Core_3(j) = (REQ_Voltages_Ferrite_Core_3(j)^2)/(2*
    REQ(j));

end

Currents_Ferrite_Core_4 = zeros(3,3);
REQ_Currents_Ferrite_Core_4 = zeros(7,1);
REQ_Voltages_Ferrite_Core_4 = zeros(7,1);
REQ_Powers_Ferrite_Core_4 = zeros(7,1);

for j = 1:7

A = Rp1 + 1i*w*Lp1;
B = 1i*w*M12_Ferrite_Core_4(j);
C = 1i*w*M13_Ferrite_Core_4(j);
```

```
D = 1i*w*M21_Ferrite_Core_4(j);
E = Rs + 1i*(w*Ls - (1/(w*Cs)));
F = 1i*w*M23_Ferrite_Core_4(j);

G = 1i*w*M31_Ferrite_Core_4(j);
H = 1i*w*M32_Ferrite_Core_4(j);
I = Rp2 + 1i*w*Lp2 + (REQ(j)*(1/(1i*w*Cp2)))/((REQ(j)+(1/(1i*w*Cp2))));

syms I1 I2 I3
eqn1 = A*I1 + B*I2 + C*I3 == V1;
eqn2 = D*I1 + E*I2 + F*I3 == V2;
eqn3 = G*I1 + H*I2 + I*I3 == V3;

[A,B] = equationsToMatrix([eqn1, eqn2, eqn3], [I1, I2, I3]);

X = linsolve(A,B);

Currents_Ferrite_Core_4(j,1) = X(1);
Currents_Ferrite_Core_4(j,2) = X(2);
Currents_Ferrite_Core_4(j,3) = X(3);

Z = abs((REQ(j).*(1/(1i*w*Cp2)))./((REQ(j)+(1/(1i*w*Cp2)))));

REQ_Currents_Ferrite_Core_4(j) = abs(Currents_Ferrite_Core_4(j,3))*Z/
    REQ(j);
REQ_Voltages_Ferrite_Core_4(j) = REQ_Currents_Ferrite_Core_4(j) * REQ(j
    );
REQ_Powers_Ferrite_Core_4(j) = (REQ_Voltages_Ferrite_Core_4(j)^2)/(2*
    REQ(j));

end

Currents_Ferrite_Core_5 = zeros(3,3);
REQ_Currents_Ferrite_Core_5 = zeros(7,1);
REQ_Voltages_Ferrite_Core_5 = zeros(7,1);
REQ_Powers_Ferrite_Core_5 = zeros(7,1);
```

```
for j = 1:7

A = Rp1 + 1i*w*Lp1;
B = 1i*w*M12_Ferrite_Core_5(j);
C = 1i*w*M13_Ferrite_Core_5(j);

D = 1i*w*M21_Ferrite_Core_5(j);
E = Rs + 1i*(w*Ls - (1/(w*Cs)));
F = 1i*w*M23_Ferrite_Core_5(j);

G = 1i*w*M31_Ferrite_Core_5(j);
H = 1i*w*M32_Ferrite_Core_5(j);
I = Rp2 + 1i*w*Lp2 + (REQ(j)*(1/(1i*w*Cp2)))/((REQ(j)+(1/(1i*w*Cp2))));

syms I1 I2 I3
eqn1 = A*I1 + B*I2 + C*I3 == V1;
eqn2 = D*I1 + E*I2 + F*I3 == V2;
eqn3 = G*I1 + H*I2 + I*I3 == V3;

[A,B] = equationsToMatrix([eqn1, eqn2, eqn3], [I1, I2, I3]);

X = linsolve(A,B);

Currents_Ferrite_Core_5(j,1) = X(1);
Currents_Ferrite_Core_5(j,2) = X(2);
Currents_Ferrite_Core_5(j,3) = X(3);

Z = abs((REQ(j).*(1/(1i*w*Cp2)))./((REQ(j)+(1/(1i*w*Cp2)))));

REQ_Currents_Ferrite_Core_5(j) = abs(Currents_Ferrite_Core_5(j,3))*Z/
    REQ(j);
REQ_Voltages_Ferrite_Core_5(j) = REQ_Currents_Ferrite_Core_5(j) * REQ(j
    );
REQ_Powers_Ferrite_Core_5(j) = (REQ_Voltages_Ferrite_Core_5(j)^2)/(2*
    REQ(j));

end
```

```
F = (1000*REQ_Powers_Ferrite_Core_1);
F1 = (1000*Ferrite_Core_Config_1_Powers);
G = (1000*REQ_Powers_Ferrite_Core_2);
G1 = (1000*Ferrite_Core_Config_2_Powers);
H = (1000000*REQ_Powers_Ferrite_Core_3);
H1 = (1000000*Ferrite_Core_Config_3_Powers);
I = (1000000*REQ_Powers_Ferrite_Core_4);
I1 = (1000000*Ferrite_Core_Config_4_Powers);
J = (1000000*REQ_Powers_Ferrite_Core_5);
J1 = (1000000*Ferrite_Core_Config_5_Powers);

figure(6)
semilogx(REQ(3:7), F(3:7),'red')
hold on
semilogx(REQ(3:7), F1(3:7),'blue')
hold off
title('Ferrite-Core System Configuration I')
subtitle('Output Power v. Load Resistance')
xlabel('Resistance [\Omega]')
ylabel('Power [mW]')
legend('Model Data','Experimental Data', 'Location', 'northeast')

figure(7)
semilogx(REQ(3:7), G(3:7),'red')
hold on
semilogx(REQ(3:7), G1(3:7),'blue')
hold off
title('Ferrite-Core System Configuration II')
subtitle('Output Power v. Load Resistance')
xlabel('Resistance [\Omega]')
ylabel('Power [mW]')
legend('Model Data','Experimental Data', 'Location', 'northeast')

figure(8)
semilogx(REQ(3:7), H(3:7),'red')
hold on
semilogx(REQ(3:7), H1(3:7),'blue')
hold off
```

```
title('Ferrite-Core System Configuration III')
subtitle('Output Power v. Load Resistance')
xlabel('Resistance [\Omega]')
ylabel('Power [\mu W]')
legend('Model Data','Experimental Data', 'Location', 'northeast')

figure(9)
semilogx(REQ(3:7), I(3:7),'red')
hold on
semilogx(REQ(3:7), I1(3:7),'blue')
hold off
title('Ferrite-Core System Configuration IV')
subtitle('Output Power v. Load Resistance')
xlabel('Resistance [\Omega]')
ylabel('Power [\mu W]')
legend('Model Data','Experimental Data', 'Location', 'northeast')

figure(10)
semilogx(REQ(3:7), J(3:7),'red')
hold on
semilogx(REQ(3:7), J1(3:7),'blue')
hold off
title('Ferrite-Core System Configuration V')
subtitle('Output Power v. Load Resistance')
xlabel('Resistance [\Omega]')
ylabel('Power [\mu W]')
legend('Model Data','Experimental Data', 'Location', 'northeast')

%% Misc. Math

D_13 = [0.2 : 0.2 : 1];

Air_Mod_1kPower = 1000*[REQ_Powers_Air_Core_1(4), REQ_Powers_Air_Core_2
    (4), REQ_Powers_Air_Core_3(4), REQ_Powers_Air_Core_4(4),
    REQ_Powers_Air_Core_5(4)];
Air_Exp_1kPower = 1000*[Air_Core_Config_1_Powers(4),
    Air_Core_Config_2_Powers(4), Air_Core_Config_3_Powers(4),
    Air_Core_Config_4_Powers(4), Air_Core_Config_5_Powers(4)];
```

```
Ferrite_Mod_1kPower = 1000*[REQ_Powers_Ferrite_Core_1(4),
    REQ_Powers_Ferrite_Core_2(4), REQ_Powers_Ferrite_Core_3(4),
    REQ_Powers_Ferrite_Core_4(4), REQ_Powers_Ferrite_Core_5(4)];
Ferrite_Exp_1kPower = 1000*[Ferrite_Core_Config_1_Powers(4),
    Ferrite_Core_Config_2_Powers(4), Ferrite_Core_Config_3_Powers(4),
    Ferrite_Core_Config_4_Powers(4), Ferrite_Core_Config_5_Powers(4)];

figure(11)
loglog(D_13, Ferrite_Exp_1kPower,'blue')
hold on
loglog(D_13, Ferrite_Mod_1kPower,'cyan')
loglog(D_13, Air_Mod_1kPower,'magenta')
loglog(D_13, Air_Exp_1kPower,'red')
hold off
title('Relative Performance at 1k\Omega')
subtitle('Output Power v. Distance between TX and RX')
xlabel('Distance [m]')
ylabel('Power [mW]')
legend('Ferrite Experimental Data','Ferrite Model Data','Air Model Data
    ','Air Experimental Data', 'Location', 'northeast')
```

VIII Acknowledgment

I would like to thank Dr. David Burnett for his patience, flexibility, and technical expertise throughout the long and arduous completion of this thesis. Additionally, I would like to thank the Honors College faculty, particularly Dr. Yasmeen Hanoosh, Dr. Jesse Hoffman, Mrs. Brianna Avery, and Mrs. Cornelia Coleman for helping me with the various administrative issues I faced. Hopefully, the quality of this work will reflect their efforts in working with me to create the best thesis possible.

IX References

[1] Patrick P. Mercier, and D. Lee, “Introduction to Ultra Low Power Transceiver Design,” in ULTRA-LOW-POWER SHORT-RANGE RADIOS, SPRINGER INTERNATIONAL PUBLISHING, 2016.

[2] SEMTECH, “User Guide - LinkCharge™ LP Series TSWITX-5V-2RX-EVM Wireless Charging Transmitter (Rev 1.01).” SEMTECH.

[3] Z. Dong, S. Liu, X. Li, Z. Xu, and L. Yang, “A novel long-distance wireless power transfer system with constant current output based on domino-resonator,” IEEE Journal of Emerging and Selected Topics in Power Electronics, vol. 9, no. 2, pp. 2343–2355, 2021.

[4] D. C. Burnett, H. M. Fahad, L. Lee, F. Maksimovic, B. Wheeler, O. Khan, A. Javey, and K. S. Pister, “Two-Chip Wireless H2S Gas Sensor System Requiring Zero Additional Electronic Components,” 2019 20th International Conference on Solid-State Sensors, Actuators and Microsystems and Eurosensors XXXIII (TRANSDUCERS and EUROSENSORS XXXIII), 2019.

[5] F. Wen, X. Chu, Q. Li, R. Li, L. Liu, and F. Jing, “Optimization on Three-Coil Long-Range and Dimension-Asymmetric Wireless Power Transfer System,” IEEE Transactions on Electromagnetic Compatibility, vol. 62, no. 5, pp. 1859–1868, 2020.

[6] M. Wang, J. Feng, Y. Shi, and M. Shen, “Demagnetization Weakening and Magnetic Field Concentration With Ferrite Core Characterization for Efficient Wireless Power Transfer,” IEEE Transactions on Industrial Electronics, pp. 1842–1851, 2018.

[7] “Taidacent High Power 24V 200mm One-to-Many Long Distance Wireless Charging Pad Contactless Power Supply Module Can be Used for Multiple Receivers,” Amazon, 2010. [Online]. Available: https://www.amazon.com/gp/product/B07QNF6J6Z/ref=ppx_yo_dt_b_asin_title_o00_s00?ie=UTF8&psc=1. [Accessed: 12-Aug-2021].

[8] X. Zhai, H. Wang, J. Li, Z. Huang, and R. Gao, “A lightweight wireless charging method for unmanned aerial vehicles,” Journal of Physics: Conference Series, vol. 1754, no. 1, p. 012176, 2021.

[9] S. Raju, R. Wu, M. Chan, and C. P. Yue, “Modeling of mutual coupling Between Planar inductors in wireless power applications,” IEEE Transactions on Power Electronics, vol. 29, no. 1, pp. 481–490, 2014.

[10] J. Gao, G. Yan, Z. Wang, P. Jiang, and D. Liu, "A capsule robot powered by wireless power transmission: Design of its receiving coil," Sensors and Actuators A: Physical, vol. 234, pp. 133–142, 2015.

[11] P. T. Theilmann and P. M. Asbeck, "An analytical model for inductively coupled implantable biomedical devices with ferrite rods," IEEE Transactions on Biomedical Circuits and Systems, vol. 3, no. 1, pp. 43–52, 2009.

Jakob White is a BS candidate in the Electrical & Computer Engineering department at Portland State University. During the course of his research and studies, he has been involved in a breadth of electrical engineering work, from designing analog electronics to programming micro-controllers. He hopes to eventually obtain a MS degree and work on cutting-edge analog electronics.